Marine Geology
April 2018, Volume 398 Pages 1-21
https://doi.org/10.1016/j.margeo.2017.12.009
https://archimer.ifremer.fr/doc/00418/52972/

The Western Tyrrhenian Sea revisited: New evidence for a rifted basin during the Messinian Salinity Crisis

Lymer Gaël [1, 3, *], Lofi Johanna [2], Gaullier Virginie [3], Maillard Agnès [4], Thinon Isabelle [5], Sage Françoise [6], Chanier Frank [3], Vendeville Bruno Claude [3]

[1] Univ Birmingham, Sch Geog Earth & Environm Sci, Birmingham B15 2TT, W Midlands, England.
[2] Univ Montpellier 2, UMR CNRS Geosci Montpellier 5243, Batiment 22,Pl E Bataillon, F-34095 Montpellssier 05, France.
[3] Univ Littoral Cote dOpale, CNRS, Univ Lille, UMR 8187,LOG, F-59000 Lille, France.
[4] Univ Paul Sabatier, GET, OMP, 14 Av E Belin, Toulouse, France.
[5] BRGM DGR GBS, 3 Ave Claude Guillemin,BP36009, F-45060 Orleans 2, France.
[6] UMR CNRS 7329 Geoazur, 250 Rue Albert Einstein, F-06560 Valbonne, France.

* Corresponding author : Gaël Lymer, email address : g.lymer@bham.ac.uk

johanna.lofi@gm.univ-montp2.fr ; virginie.gaullier@univ-lille1.fr ; Agnes.MAILLARD-LENOIR@Get.omp.eu ; i.thinon@brgm.fr ; francoise.sage@ekope.com ; frank.chanier@univ-lille1.fr ; Bruno.Vendeville@univ-lille1.fr

Abstract :

In the last fifty years, the Messinian Salinity Crisis (MSC) has been widely investigated in the Mediterranean Sea, but a major basin remains fewly explored in terms of MSC thematic: the Western Tyrrhenian Basin. The rifting of this back-arc basin is considered to occur between the Middle-Miocene and the Early-Pliocene, thus including the MSC, giving a unique opportunity to study the crisis in a context of active geodynamics. However the MSC seismic markers in the Western part of the Tyrrhenian Sea have only been investigated in the early eighties and the MSC event in the Western Tyrrhenian Basin remains poorly studied and unclear.

In this study, we revisit the MSC in the Western Tyrrhenian Basin, i.e. along the Eastern Sardinian margin. We present results from the interpretation of a 2400 km long HR seismic-reflection dataset, acquired along the margin during the “METYSS” research cruises in 2009 and 2011. The maps of the MSC seismic markers reveal that the Eastern Sardinian margin was already dissected in structurals highs and lows during the MSC. We also demonstrate that the MSC markers constitute powerfull time-markers to refine the age of the rifting, which ended earlier than expected in the East-Sardinian Basin and the Cornaglia Terrace. These results allow us to discuss the palaeo water-depth of the Western Tyrrhenian Basin during the MSC, as well as implications for possibles scenarios of the Messinian Salinity Crisis across the Eastern Sardinian margin.

Highlights

► Characterization and mapping of the seismic markers of the Messinian Salinity Crisis along the Eastern Sardinian margin. ► Relations between tectonics and sedimentation in the Western Tyrrhenian Basin. ► Refining the timing of the rifting in the Western Tyrrhenian Basin. ► Morphology of the Western Tyrrhenian Basin during the Messinian Salinity Crisis. ► Evolution of the Eastern Sardinian margin from rifting to present-day.

1 INTRODUCTION

The rifting of the Western Tyrrhenian Basin is interpreted to occur from middle-Miocene times to the Early-Pliocene (Kastens et al., 1988; Mascle and Réhault, 1990; Sartori, 1990; 2003; Sartori et al., 2001; 2004; Carminati et al., 2012). Several authors thus consider Tortonian *p.p.* to Pliocene *p.p.* deposits as syn-rift sediments (Sartori et al., 2001; 2004). The Western part of the Tyrrhenian Sea (*i.e.*, the Eastern Sardinian margin, Figure 1) then constitutes a major target regarding the Messinian Salinity Crisis (MSC) problematics, as it gives a unique opportunity to study the crisis in a context of active geodynamics. However, the MSC has been fewly investigated in the Western Tyrrhenian Basin and some of the MSC seismic markers have been mapped across the Eastern Sardinian margin in the early eigthies (Curzi et al., 1980; Malinverno et al., 1981; Moussat, 1983). In addition the status of this basin during the MSC ("peripheral shallow", "intermediate" or "deep" water) is still unclear,

although it is considered as an intermediate depth depocenter equivalent to the Sicilian Caltanissetta Basin in recent studies (Roveri et al., 2014a, 2014b).

In this article we revisit the Western Tyrrhenian Basin using a recent dataset of 2400 km high-resolution seismic reflection profiles, acquired during the "METYSS 1 and 3" research cruises (**M**essinian **E**vent in the **T**yrrhenian from **S**eismic **S**tudy; Gaullier et al., 2014; Lymer, 2014). We identify the MSC seismic markers using the nomenclature defined by Lofi et al. (see the "Seismic atlas of the Messinian Salinity Crisis markers in the Mediterranean and Black seas", Lofi et al., 2011a, b) and we use them to bracket the timing of the rifting across the Eastern Sardinian margin. We finally discuss the palaeo-bathymetry of the margin during the MSC and the implications on the emplacement of the MSC seismic markers in the Western Tyrrhenian Basin.

2 GEOLOGICAL SETTING OF THE EASTERN SARDINIA MARGIN

2.1 Morphology of the study area

The study area is located in the Western Tyrrhenian Sea, along the Eastern Sardinian margin (Figure 1). The margin is segmented in three physiographic segments (Figure 1):

1. The East-Sardinia Basin (200-2000 m water depth). The Orosei Gulf area includes several canyons, which merge to form the Orosei Canyon at the transition between the East Sardinia Basin and the Cornaglia Terrace (Figure 1). North of the Orosei Gulf, the East-Sardinia Basin is 10 km to 20 km wide and is bounded eastward by the Baronie Ridge (Figure 1). South of the Orosei Gulf, the basin is up to 40 km wide and is bounded eastward by the Sardinia and Quirra Seamounts. The Sarrabus Canyon trends to the North-East from the East-Sardinia Basin to the Cornaglia Terrace along the southeast flank of the Sardinia Seamount (Figure 1);

2. The Cornaglia Terrace is a wide, flat, open area, with water depths ranging from 2000 m to 3000 m. It displays local structural highs, such as the Onifai Ridge and the Cornaglia

Seamount (Figure 1). The Orosei Canyon and its associated meandering deep channel cut this large step in an overall E-W direction (Figure 1);

3. The Tyrrhenian Basin *stricto sensu* corresponds to the deep-water domain, with water depths varying from 3000 m to 3600 m. It includes the Magnaghi Basin, which is delineated westward by the Central Fault (Réhault et al., 1987) marked by a huge bathymetric scarp underlined by the Major Seamount (Figure 1).

2.2 Geodynamics

The Tyrrhenian Sea is a Neogene back-arc basin that opened by continental rifting and oceanic spreading related to the eastward migration of the Apennine subduction system from middle Miocene to Pliocene times (Malinverno and Ryan, 1986; Gueguen et al., 1998; Jolivet and Faccenna, 2000; Sartori et al., 2001; Doglioni et al., 2004; Jolivet et al., 2006; Carminati et al., 2012; Prada et al., 2016). The opening of the Tyrrhenian Basin was part of a continuous process of lithospheric extension, which led to the opening of the whole Western Mediterranean Sea, from the Oligocene to Present-day. Extension was related to the progressive retreat of the subducting Ionian slab, coevally with the slow convergence between Africa and Europe (Malinverno and Ryan, 1986; Dewey et al., 1989; Jolivet and Faccenna, 2000; Jolivet et al., 2006; Carminati et al., 2012).

The locus of extension in the Tyrrhenian Sea is considered to migrate from West to East as it followed the eastward progressive retreat of the Apennine subduction system (Malinverno and Ryan, 1986; Kastens et al., 1988; Mascle and Réhault, 1990; Sartori, 1990; 2003; Sartori et al., 2001; 2004; Mattei et al., 2002; Jolivet et al., 2006; Carminati et al., 2012). In the southern Tyrrhenian Sea, rifting started during Serravallian-Tortonian times, and, possibly, as early as the Langhian (*c.* 16-13.8 Ma) along the Eastern Sardinian margin. The rifting ended during the Early-Pliocene with sea-floor spreading in the deep Tyrrhenian Basin, East of the Central fault (Kastens et al., 1988; Mascle and Réhault, 1990; Sartori, 1990; 2003; Sartori et

al., 2001; 2004; Carminati et al., 2012). Several authors consider Tortonian *p.p.* to Pliocene *p.p.* deposits as syn-rift sediments (Sartori et *al.,* 2001; 2004), meaning that the MSC would be syn-rift along the Eastern Sardinian margin. The extension direction during rifting was roughly E-W, as shown by the N-S trending normal faults that form the present-day stepped physiography of the study area (Figure 1) (Malinverno and Ryan, 1986; Mascle and Réhault, 1990; Sartori et al., 2001). Sartori et al. (2001) also described some transverse lineaments, such as the Orosei Canyon Line (OCL; Figure 1). The OCL has been interpreted as a transfer fault that separated the Cornaglia Terrace in two domains that have been subjected to different amounts of extension during rifting (Sartori et al., 2001).

About recent tectonic activity, Gaullier et al. (2014) and Lymer (2014) demonstrated the existence of significant post-MSC crustal deformation along the Eastern Sardinian Margin. They particularly pointed out clear crustal structures in the MSC and Plio-Quaternary brittle sedimentary strata, including both extensional and mild compressional deformations. Some of these structures locally show very recent crustal activity, probably late Quaternary in age. Plio-Quaternary deformation has affected the inner Sardinian margin (Gaullier et al., 2014), previously assumed to have experienced very weak or no recent crustal activity (Mascle and Réhault, 1990), although Curzi et al. (1980) have invoked strong post-MSC vertical motions in order to explain the present-day stepped architecture of the MSC markers accross the margin.

2.3 Sedimentary framework

Drilling results from ODP sites 654 and 653 (Leg 107) (Kastens et al., 1988; Mascle and Réhault, 1990), located respectively on the western and eastern sides of the Cornaglia Terrace (Figure 1), have provided data on the composition and age of the cored sediments and have allowed correlations with the seismic units. ODP Site 653 is located very close to the older DSDP Site 132 (Figure 1) (Ryan, 1973). Drills from the three sites reached beyond the

Miocene-Pliocene boundary, allowing for the characterization of the Plio-Quaternary and part of the MSC depositional sequence (Figure 2). Only site 654 provided cores from pre-MSC units, correlated to a vertical succession of pre-rift, syn-rift and post-rift sequences (Figure 2A).

On Site 654, we differentiate four seismic units (Figure 2). Seismic unit 4 is the oldest (Figure 2A) and corresponds to lithostratigraphic unit VI from Kastens (1992). It is made of conglomerate and iron-oxide-rich matrix attributed to continental depositional setting, such as an alluvial fan. Age of unit 4 is unknown, but it is assumed to be pre-rift (Kastens et al., 1988; Mascle and Réhault, 1990; Sartori, 1990).

Seismic unit 3 (Figure 2A) corresponds to lithostratigraphic units V and IV from Kastens (1992). Unit V corresponds to oyster-bearing glauconitic sands from nearshore shallow-water environment. Unit IV is a nannofossil chalk sequence showing a fully marine environment. Age of unit IV is Tortonian to Early Messinian (Figure 2A), based on benthic foraminiferal assemblages (Kastens et al., 1988; Mascle and Réhault, 1990). Thus, lithostratigraphic units VI, V and IV have recorded an evolution from restricted marine to open deep marine environments, attributed to the rifting of the margin (Kastens et al., 1988; Mascle and Réhault, 1990; Kastens, 1992), which is consistent with the fan-shaped geometry of seismic unit 3, associated with a crustal normal fault visible westward of the drill site on the MYS12 seismic line (Figure 2A). It shows that a large amont of tectonic subsidence occurred before the MSC (Kastens et al., 1988; Kastens, 1992).

Seismic unit 2 corresponds to the lithostratigraphic units III and II from Kastens (1992), both related to the MSC. Lithostratigraphic unit III is made of finely-layered claystone and siltstone rich in organic carbon, dolomite and siliceous fossils such as radiolarians, diatoms and sponge spicules, but with rare or absent foraminifera and no calcareous nannoplankton. The evaporitic free lithostratigraphic unit III is interpreted as a “salinity crisis lithofacies”

that marks the onset of restricted marine conditions related to the MSC, deposited in a low-energy setting and associated with a high degree of evaporation in the waters (Kastens et al., 1988; Kastens, 1992). Lithostratigraphic unit III is considered by Kastens et al. 1988 as being syn-rift on the base of the presence of micro-faults within the fine sedimentary layers, but this same unit is not considered as syn-rift anymore by Kastens (1992). The syn-rift deposition of lithostratigraphic unit III will be discussed in section 6.2.1. Lithostratigraphic unit II is characterized by cycles of gypsum rich intervals interbedded with gypsum poor layers made of clays, mudstone and minor nanofossil ooze containing dwarf organisms of Messinian age. The evaporitic lithostratigraphic unit II is interpreted as being accumulated during the MSC desiccation event and is considered to be post-rift (Kastens et al., 1988; Cita et al., 1990; Kastens, 1992). In a recent stratigraphic revision of the sedimentary facies cored at ODP site 654, Roveri et al. (2014a) and Lugli et al. (2015) interpreted the lithostratigraphic unit III as an evaporitic free unit commonly deposited in deeper settings along the Apennine orogenic wedge, while the first evaporitic deposits, the Primary Lower Gypsum (PLG), contemporaneously accumulated in shallower settings (see section 3.1) after the onset of the MSC. Above, the lithostratigraphic unit II is considered to correspond to the Resedimented Lower Gypsum (RLG) and the Upper Gypsum (UG) succession (Roveri et al., 2014a), accumulated in intermediate depth setting (see section 3.2) during later stages of the MSC. A gypsum-layered unit with dwarf nannofossils of Messinian age was also encountered at sites 653 and 132 (Figure 2; Kastens et al., 1988; Cita et al., 1990). The seismic unit 2 correlates on the seismic lines with strong, sub-parallel reflectors that we interpret to be MSC evaporites, for instance the Upper Unit (UU; Figure 2), a characteristic MSC seismic marker defined by Lofi *et al*. (2011a and b; see section 3.3).

The seismic unit 1 is the youngest and corresponds to lithostratigraphic unit I from Kastens (1992). It consists of hemipelagic sequences dominated by nanofossils and foraminiferal ooze

(Unit 1, Figure 2). The age of this unit is Plio-Pleistocene (Kastens et al., 1988; Mascle and Réhault, 1990). Drilling at Site 654 moreover encountered a thin basalt layer located near the Pliocene-Pleistocene boundary (Kastens et al., 1988). This layer corresponds to a highly reflective horizon on the MYS12 seismic line (Figure 2A). Seismic units 1 and 2 are attributed to the post-rift sequence, which means that the syn-rift/post-rift transition at sites 654 took place during Early Messinian times (Kastens et al., 1988; 1992; Mascle and Réhault, 1990).

3 THE MESSINIAN SALINITY CRISIS IN THE WESTERN MEDITERRANEAN BASINS

Less than 6 My ago, the Mediterranean Sea underwent rapid and dramatic paleo-environmental changes during the Messinian Salinity Crisis (MSC) (Hsü et al., 1973). This short-term episode at the geological scale (~5.97-5.33 Ma, Krijgsman et al., 1999a; Manzi et al., 2013) involves several possible scenarios still debated nowadays, including numerous open questions regarding the succession of events during the crisis (see Rouchy and Caruso, 2006; CIESM, 2008; Lofi et al., 2011a, b; Roveri et al., 2014b; Roveri et al., 2016). A commonly considered scenario implies high-amplitude (> 1500 m) sea-level oscilations of the Mediterranean (Hsü et al., 1973; Ryan and Cita, 1978), resulting in strong sub-aerial erosion of the Mediterranean margins (Clauzon, 1973; Ryan and Cita, 1978; Lofi et al., 2005), while MSC deposits (mainly evaporites) accumulated in the deepest settings (Montadert et al., 1970; Hsü et al., 1973; Lofi et al., 2005; 2011a, b). Alternatively, other scenarios consider a persistent Mediterranean water body and the erosion of the margins as a result from both subaerial and subaqueous tracts (Roveri et al., 2014c; 2016). A common feature of MSC scenarios is the distinction of statuses, in term of paleo-bathymetry, for the MSC basins (*e.g.* Rouchy and Caruso, 2006; CIESM, 2008; Lofi et al., 2011a, b; Roveri et al., 2014a, b; Roveri et al., 2016). In this study we differentiate three distinct statuses (Figure

3) based on the relative depth between the different basins, but mainly on the presence/absence of specific seismic units: 1) the peripheral shallow basins, 2) the intermediate basins, and 3) the deep basins. Define the status of the MSC basins is crucial regarding the connections/disconnections, and therefore the correlations, between those different basins during the MSC. In this context, intermediate basins (Figure 3), as is sometimes interpreted the Western Tyrrhenian Basin (Roveri et al., 2014a, b), are considered as key areas to correlate peripheral and deep basins and define the timing of the MSC events in a global MSC scenario (CIESM, 2008).

3.1 Peripheral shallow basins

The peripheral shallow basins (Figure 3) are thought to have water depths of less than 200 m and to be partly isolated from the deep basins. They have been mostly emerged and eroded during the MSC (Clauzon et al., 1996; Rouchy and Caruso, 2006; CIESM, 2008; Lofi et al., 2011b). The 5.97 Ma onset of the MSC has been defined in the peripheral shallow basins (Krijgsman et al, 1999a, b), marked by a synchronous decrease and eventually the disappearance of the normal marine biota (Manzi et al., 2013), later followed by the precipitation of the first evaporitic deposits, the ***Primary Lower Gypsum (PLG)*** (Roveri et al., 2014b, 2016). Filamentous microfossils found in the PLG have been interpreted either as fossil cyanobacteria remains (Panieri et al., 2010), thus constraining the water depth in the peripheral basins to above the photic zone, or as fossil sulphide oxidizing bacteria remains (Dela Pierre et al., 2015), allowing gypsum formation at water depth greater than 200 m, in agreement with the work of Ochoa et al. (2015) on the Balearic promontory. In this study, we consider peripheral shallow basins as basins showing evidence for the presence of PLG only (Figure 3), overlain by Pliocene deposits. In term of water depths, these can exceed 200 m. In term of seismic records, some ***Bedded Units (BU)*** of Lofi *et al*. (2011), comformable at the

base and eroded at the top, are considered to be composed of PLG (Driussi et al., 2015; Ochoa et al., 2015; Rossi et al., 2015).

3.2 Intermediate basins

Sicily is often considered as locally being an intermediate basin, now outcropping onshore as a result of tectonics. The oldest MSC deposits consist in evaporite-free, barren deposits, interpreted as the deeper contemporaneous equivalent of the PLG (Dela Pierre et al., 2011; Roveri et al., 2014b, 2016 and references therein). Above, the MSC evaporitic products consist of ***Resedimented Lower Gypsum (RLG)***, containing halite and clastic gypsum derived from the erosion of the PLG, overlain by the ***Upper Gypsum (UG).*** Finally, brackish deposits (Lago Mare) mark the end of the record of the MSC (Roveri et al., 2008, Roveri et al., 2014a; Caruso et al., 2015; Popescu et al., 2015; Roveri et al., 2016). Interpreted as deep settings of peripheral shallow basins in previous publications (e.g. CIESM 2008, Roveri et al., 2014a, b), intermediate basins are often considered as lying between 200m (peripheral basins) and 1000m (deep basins) of water depth during the MSC (Roveri, et al., 2014 a, b). These bathymetries are however somehow arbitrary and, as discussed above, some of them debated. In this study (Figure 3), we thus consider the intermediate basins as located between peripheral shallow basins (presence of PLG only) and deep basins (presence of thick halite, overlained by UU in the western basin) (Lofi et al., 2011a; Maillard and Mauffret, 2011). In term of seismic records, intermediate basins contain either some BU, concordant or uncomformable at the base and at the top (Lofi et al., 2011a; Driussi et al., 2015; Maillard et al., 2014; Thinon et al., 2016), or an incomplete record of the deep basin trilogy such as the aggrading ***Upper Unit (UU)*** (Valencia trough, Maillard et al., 2006). In our view, intermediate depth basins thus cover a wide range of both bathymetries and MSC deposits (either BUs or CUs), which do not necessarily have the same ages and associated depositional environements.

3.3 Deep basins

Deep basins correspond to basins whose rifting was finished before the MSC (*e.g.* the Algero-Provençal Basin; Gueguen et al., 1998; Jolivet and Faccenna, 2000; Jolivet et al., 2006). They were located offshore in the deep Mediterranean areas, with water depth exceeding 1000 m before the MSC (Figure 3; CIESM, 2008). They accumulated thick deposits during the MSC (Rouchy and Caruso, 2006; CIESM, 2008 and references therein; Lofi et al., 2011a, b; Roveri et al., 2014a, b) comprising clastic units and thick evaporites (including thick salt layer), belonging to the "Messinian trilogy" in the western basin (Montadert et al., 1970; CIESM, 2008; Lofi et al., 2011a, b).

In the recent nomenclature defined by Lofi et al. (2011a, b), the MSC depositional units of the western Mediterranean deep basins correspond from the base to the top to:

The Lower Unit (LU) (Figure 3)***:*** Located below the mobile salt, it is considered as the oldest unit of the Messinian trilogy, although it has never been drilled and its age and exact lithology remains unknown (Lofi et al., 2005; Lofi et al., 2011a and 2011b).

The Mobile Unit (MU) (Figure 3)***:*** This unit displays a transparent seismic facies and corresponds to the main salt layer of the MSC, mainly constituted of halite, which deforms ductilly and generates salt tectonics (*e.g.* Obone-Zue-Obame et al., 2011; Gaullier et al., 2014). Where non-deformed, the MU has an estimated thickness of about 1200 m in the Western Mediterranean Basin (assuming an internal seismic velocity of 4.5 km/s, Lofi et al., 2011b).

The Upper Unit (UU) (Figure 3)***:*** Located above the MU, the UU is the youngest unit of the MSC in the Western Mediterranean Basin. It corresponds to high-amplitude, parallel reflectors onlapping the Miocene margins. Its thickness locally reaches up to 700 m (assuming an internal seismic velocity of 3.5 $km.s^{-1}$, Lofi et al., 2011a). Data from DSDP and ODP drillings show that its top is composed of alternating marls and evaporites. The UU

potentially includes significant quantities of clastic material near the MSC canyons (Sage et al., 2005; Maillard et al., 2006; Lofi et al., 2011b).

The Complex Unit (CU) (Figure 3): This unit has a chaotic or roughly-bedded seismic facies resulting from the MSC erosion of the margins and has been deposited at the slope-basin transition (Lofi et al., 2005; Maillard et al., 2006; Lofi et al., 2011a and b; Obone-Zue-Obame et al., 2011). All CUs do not necessarily have the same age and emplacement mechanisms. The nomenclature of Lofi et al. (2011a, b) also includes several remarkable MSC surfaces defined on the basis of their geometric relationship with the pre-MSC units, the MSC units and the Plio-Quaternary sedimentary cover:

The Margin Erosion Surface (MES) (Figure 3) affects all Mediterranean margins (Mauffret et al., 1978; Ryan and Cita, 1978; Guennoc et al., 2000; Lofi et al., 2003 ; Lofi et al., 2005; Lofi et al., 2011b). On the seismic profiles, this surface corresponds to an unconformity between pre-MSC and Pliocene deposits. Its origin is interpreted as either resulting from sub-aerial erosion, essentially through the retrogressive erosion of rivers (Stampfli and Höcker, 1989; Loget and Van Den Driessche, 2006; Urgeles et al., 2011), or recording both subaqueous and subaerial erosional processes (Lofi et al., 2005; Cameselle and Urgeles, 2017), through wave ravidement (Bache et al., 2009; Garcia et al., 2011), slope failures and gravity flows (Roveri et al., 2016).

The Bottom Surface (BS) and ***The Top Surface (TS)*** (Figure 3) constitute conformable surfaces, respectively at the bottom and the top of the MSC deposits (Ryan and Stanley, 1971; Mauffret et al., 1973). Locally, they show evidence of erosion (Lofi et al., 2005; Bertoni and Cartwright, 2006; Maillard et al., 2006; Thinon et al., 2016) and are then labelled ***Bottom Erosion Surface (BES)*** and ***Top Erosion Surface (TES)***.

4 DATA SET AND METHODOLOGY

4.1 Seismic data

For this study, 50 high-resolution seismic profiles (~2400 km) have been acquired along the Eastern Sardinian margin, onboard the R/V "Téthys II" (INSU-CNRS) during the "METYSS 1" and "METYSS 3" cruises, in June 2009 (Gaullier et al., 2014) and April 2011 (Figure 1). The seismic system was a mini-GI (SODERA) air gun and a 6-channel 25 m streamer. The profiles obtained were processed using the Géovecteur© software package. The processing sequence aimed at improving the signal-to-noise ratio, and included the following steps: Common Mid-Point (CMP) gathering, gain recovery, normal moveout correction using variable velocity, CMP-stack (fold of coverage of 6), post-stack Kirchhoff migration, and time-variable frequency filtering. Because of the seismic device used during the METYSS survey, the maximum offset did not exceed 250 m, so that no velocity model can be inferred from our dataset. With no velocity information, the main purpose of seismic migration was to focus most of the diffraction artifacts that typically hide the salt diapir flanks. Tests on the migration velocities have indicated that the hyperbolas best focus for RMS-velocities of 1500 m/s on the margin, and for velocities ranging between 1500 m/s and 1700 m/s within the deep basin, where there are salt diapirs.

4.2 Methodology

The seismic lines were interpreted according to the rules of seismic stratigraphy (Mitchum and Vail, 1977). When identified, the MSC markers were correlated across the study area and subsequently mapped using the Kingdom suite© software package. When presented in meter, the depths and thicknesses of the different units were obtained by converting time to depth using typical values for the internal seismic velocities of the different units, namely: 1500 m/s for the water column, 1800 to 2200 m/s for the Pliocene-Quaternary overburden, 3500 m/s for the Upper Unit, and 4500 m/s velocity for the Mobile Unit (Réhault et al., 1984). The

seismic line MYS12 (Figure 2A) was acquired in the the vicinity of the ODP site 654 (Figure 1) and shows the same seismic succession than the one observed by Kastens et al. (1988) and Mascle and Réhault (1990) in this area of the margin, allowing to project the ODP site 654 on the METYSS dataset.

5 MAIN RESULTS

The interpretation of the "METYSS" seismic profiles enabled us to identify the following seismic units and surfaces.

5.1 Post-MSC units: Pliocene-Quaternary

The most recent unit along the Eastern Sardinian margin corresponds to the Plio-Quaternary, labelled "PQ", which overlays the MSC seismic markers (Figures 4, 5). The PQ unit is either split into two sub-units having different seismic facies, or is locally homogeneous. Where the two sub-units are observable, the oldest one is characterized by continuous reflectors of low to moderate amplitude. The reflectors are either sub-parallel (Figure 5) or locally divergent (Figure 6, CDP 1100 to 1800). This sub-unit is considered to be Early-Pliocene in age, since it directly overlains the MSC seismic markers. The most recent PQ sub-unit is considered to be intra-Pliocene to present-day in age (Sartori et al., 2001). It displays continuous parallel and well-bedded reflectors. Both sub-units are locally separated by an angular unconformity (purple line on Figures 6 and 7, Gaullier et al., 2014).

5.2 Pre-MSC units

The oldest terranes observed on the seismic lines are labeled “pre-MSC” and include the Hercynian basement, some sedimentary units from Jurassic to Miocene in age, or magmatic material (Curzi et al., 1980; Mascle and Réhault, 1990; Sartori, 1990; Sartori et al., 2001). The pre-MSC units are best visible where the MSC units are thin or absent (Figures 4, 5 and 6). Locally, we can differentiate several types of pre-MSC reflectors on the basis of their geometries. One such example is illustrated by Figure 4 (pink and blue horizons).

The pink horizons appear sub-parallel and significantly tilted toward the East (Figures 4 and 6). We consider the age of the pink horizons to be pre-MSC. Indeed, our pink unit correlates well with the sub-unit B3.2 interpreted by Sartori et al. (2001), which has been sampled on the Sardinia Seamount (core BS77-19, Figures 1 and 6) and dated from Tortonian *s.l.* age. In addition, where observed, the pink horizons are truncated (Figures 4, 5 and 6), either by the MES or the BES, which is coherent with a pre-MSC age of the deposits which would have been eroded during the MSC. Specifically, below the Sardinia Seamount (Figure 6), the pink reflectors are eroded both eastward and the westward, showing the spectacular erosive characteristic of the MES. One could argue that the pink horizons correspond to the PLG, whose top is marked with the MES. However we do not think the pink horizons correspond to the seismic signature of evaporites. In addition the deposition of the pink unit on the flanks of the present-day basins (Figures 4 and 6), while the MSC units accumulated in the deepest parts of the present-day basins, suggest a switch in the location of the depocenters between the two units, requiring a certain amount of time that is also consistent with a pre-MSC emplacement of the pink unit.

Where observable, blue reflectors present a clear fan-shaped geometry associated with crustal normal faults (Figures 2A, 4 and 5). This strongly support that the blue horizons correspond to the syn-rift deposits. On the continental slope and on the Quirra Seamounts, the age of syn-rift deposits is unknown, but the blue reflectors are located below the pink reflectors and below the MSC seismic markers (Figures 4 and 5). The blue syn-rift horizons are therefore unambiguously pre-MSC in age. According to the estimated age of the pink unit on the Sardinia Seamount (Sartori et al., 2001), the age of the syn-rift deposits could be contained somewhere between the beginning of the Miocene and part of the Tortonian, or the Langhian (Carminati et al., 2012). At Site ODP 654, the blue reflectors also display a fan-shaped geometry (Figure 2A) and have been dated to be Late Tortonian to Earliest Messinian in age

(Kastens et al., 1988; Mascle and Réhault, 1990). Moreover, on figures 4 and 5, crustal normal faults do not affect the MSC markers, implying that crustal tectonics activity of these faults stopped before the MSC and confirming that the syn-rift period is pre-MSC.

5.3 MSC seismic markers: Messinian surfaces

We labelled the MSC surfaces according to the nomenclature of the Seismic Atlas of the MSC (Lofi et al., 2011a).

5.3.1 Margin Erosion Surface (MES)

On the Eastern Sardinian margin, the MES corresponds to a high-amplitude reflector. The truncation of underlying pre-MSC reflectors shows that this is an erosion surface (Figures 4 and 6). It can be attributed to the MES, because it is laterally geometrically connected to the MSC deposits (Figures 5, 6, 7, 8, 9).

5.3.1.1 The East-Sardinia Basin

The MES progressively deepens from the coast towards the East-Sardinia Basin (Figure 10). Upslope the MES displays rough and valley-like morphologies (Figures 4 and 6). The Early-Pliocene deposits, or PQ deposits where the sequence is homogeneous, directly fill the MSC paleo-valleys (Figures 4 and 6). The depth of incision of the MSC valleys is generally less than 110 m, although one major valley has incised the pre-MSC series by approximately 280 m (Figure 4, CDP 1740). Downslope, the MES is markedly smoother. It passes laterally to the BS/BES and TS/TES where the deep basin MSC deposits onlap the slope (Figures 6, 9 and 10).

5.3.1.2 The Cornaglia Terrace

The present-day bathymetry of the studied area is marked by several structural highs (Quirra Seamounts, Sardinia Seamount, Baronie, Caprera and Onifai Ridges), particularly at the transition between the East-Sardinia Basin and the Cornaglia Terrace (Figure 1). On top of these highs, the observed erosion surface is interpreted as being the MES (Figure 10) because

it laterally passes in some places to the BS/BES and TS/TES (for instance the top of the UU on Figures 5, 6 CDP 1300 and 3070, 7 and 8). The MES deepens from the top of the highs toward the surrounding basins (Figure 10). The Early-Pliocene deposits lie directly onto the MES, as it is the case on the flanks of the East-Sardinia Basin (Figure 6).

At the top of isolated structural highs, such as the Cornaglia Seamount (Figure 10), the observed erosion surface cannot be undoubtedly attributed to the MES and is then labelled as "probable MES" (Figure 10). The structural disconnection between the erosion surface and the MSC deposits (Figure 11), does not allow constraining the age of the erosion. Netherveless, we interpret this surface as being the MES because the MSC units (UU and MU) pinch out at the foot of the structural highs, suggesting that no MSC sediments were deposited on the highs (Figure 11). In addition, local dredges from the top of the Cornaglia Seamount and the Baronie Ridge provided samples from the Variscan basement, with neither MSC nor PQ strata (Sartori et al., 2001; 2004). Where the Early-Pliocene series are absent, it remains difficult to confirm the age of the erosion surface. Indeed, the surface could be pre-MSC in age, and/or have been reactivated later during Plio-Quaternary times. However, the MSC is the most probable last event at the origin of an erosion surface in the study area.

5.3.2 Bottom Surface/Bottom Erosion Surface (BS/ BES) - Top Surface/ Top Erosion Surface (TS/ TES)

The BES/BS is generally difficult to observe where the MU is thick, as both the base of the MU and pre-MSC units are poorly imaged on our seismic data. We can detect the BS only where the salt is relatively thin. Locally, the BS shows signs of erosion (truncated pre-MSC reflectors) and is labeled BES (Figures 5 and 6). At the edges of the basins, the BES is an unconformity between pre-MSC series and the onlaping UU (Figures 5, 6 and 11). It locally continues below the pinch-out of the MU (Figure 7). The TS constitutes a continuous

conformable high amplitude reflector (Figure 5). Locally, the TS shows evidence of erosion (truncated reflectors in the Upper Unit) and is labeled TES (Figure 5, CDP 3700 to 4600).

5.4 MSC markers: Messinian units

5.4.1 The Upper Unit (UU)

The UU roughly corresponds to the lithostratigraphic unit II from Kastens (1992), to the "upper sequence" of Curzi et al. (1980) and the seismic facies n°2 of Moussat (1983). The UU appears as a group of sub-parallel reflectors of high-frequency and high-amplitude seismic facies (Figures 5, 8 and 11). The UU is either located above the MU or onlaps the BES at the edges of the basins (Figure 11, CDP 5000) and is the most regionally widespread MSC unit visible across the Eastern Sardinian margin. It has been deposited in the basins located between the structural highs (Figure 10). The MSC related age and the lithology of the UU have been confirmed by the ODP drillings on Sites 653 and 654 (Figures 1 and 2; Kastens et al., 1988; Mascle and Réhault, 1990).

5.4.1.1 The East-Sardinia Basin

In the East-Sardinia Basin (Figure 10), the UU is an aggrading unit that laterally onlaps onto the foot of the bounding structural highs (*e.g.* the Quirra Seamounts; Figure 5). In the northern part of the East-Sardinia Basin, west of the northern tip of the Baronie Ridge, the thickness of the UU decreases from the center of the basin toward the edges (Figure 12). The TS/TES becomes progressively shallower from the center to the edges of the basin (Figure 10): We observe the top of the UU at 3.1 stwtt depth (~2550 m) in the center of the basin (Figure 7, CDP 5450) and at about 2.5 stwtt depth (1800 m) where the UU pinches out (Figure 7 CDP 3500). Northward, the UU thins much toward the East-Corsica Basin (Figure 12). It is locally 0.02 stwtt thick, *i.e.* 35 m. There, the top of the UU is eroded and shallow (Figure 10), less than 2 stwtt depth (~1300 m) (Figure 9 CDP 4150 to 6700).

In the Southern East-Sardinia Basin, we observe the thickest UU (0.23 stwtt, ~ 400 m) south of the Sardinia Seamount (Figure 12). Elsewhere west of the Sardinia and Quirra Seamounts, the thickness of the UU is roughly less than 0.15 stwtt (~260 m; Figure 12). The top of the UU deepens at the present time from the south toward the Orosei Gulf (Figure 10): We observe the top of the UU at 2.6 stwtt depth (~2000 m) against the Quirra Seamounts (Figure 5, CDP 2650); Northward, the UU onlaps the western flank of the Sardinia Seamount at 3 stwtt depth (*i.e.* ~2500 m; Figure 6, CDP 1770).

5.4.1.2 The Orosei Canyon area

The seismic facies of the UU looks unusual near the Orosei Canyon, north and northeast of the Sardinia Seamount (Figures 12 and 13), where it corresponds to several continuous, parallel, high-amplitude, and medium-frequency reflectors (Figure 13D). It also includes some local lenticular transparent sections (Figure 13C) and internal unconformities. We interpret this unit as belonging to the UU because it is located above the MU (Figure 13) and laterally related with the MES on the Sardinia Seamount (Figure 6, eastern part). However we labelled it as "chaotic UU" because we support that its particular seismic facies shows that the lithology is probably made of evaporites and a higher proportion of clastic deposits compared to the classic UU. This can be explained by the proximity of the Orosei Canyon, as observed in the vicinity of main Messinian outlets on the Northern Ligurian margin by Sage and Déverchère (2011) and on the Western Sardinia margin by Sage et al. (2005, 2011). Along these margins, the products of erosion are directly incorporated in the MSC deposits, UU and MU, close to the canyons (Sage et al., 2005; Lofi et al., 2011a). In such cases, the seismic facies of the UU appears very similar to the seismic facies observed in the Orosei Canyon area. In addition, this area is enclosed between several structural highs that have been eroded and where we observe the MES (Figure 12). The Orosei Canyon area could thus have accumulated products of erosion from the surrounding highs.

South of the Baronie Ridge, in front of the Orosei Gulf, the chaotic UU is thick (> 500 m, Figure 12). It thins out toward the surrounding structural highs, where the unit pinches off (Figure 6 and 12). The top of the chaotic UU deepens toward the northern part of the East-Sardinia Basin and the Cornaglia Terrace in the southeast (Figure 10), whereas it becomes shallower toward the structural highs (Figure 10). Figure 13 shows several normal faults affecting the chaotic UU and rooted at depth on the MU. We assume that these faults are related to salt tectonics, *i.e.* gravity gliding along the basement slope (*e.g.*, Vendeville and Cobbold, 1987; Cobbold et al., 1989).

5.4.1.3 *The Cornaglia Terrace*

On the eastern foot of the Baronie Ridge, in the northern part of the Cornaglia Terrace, the UU accumulated in isolated troughs (Figure 12) where the UU is thin, roughly < 0.15 stwtt (*i.e.*, < ~260 m). The top of UU deepens eastward across the northern part of the Cornaglia Terrace: In a trough located between the Baronie and Onifai Ridges, the UU pinches-out at 2.9 stwtt depth (*i.e.*, 2125 m, Figure 8, CDP 2200); Previous works by Moussat (1983) show that the UU extends east of the Onifai Ridge, until the ODP site 653 (Figure 12), where the UU is thin (0.12 stwtt, *i.e.*, 210 m) and the TS lies at 4 stwtt depth (*i.e.*, 3060 m; Figure 2B, CDP 4140).

In the southern part of the Cornaglia Terrace, the UU extends from the eastern side of the Quirra Seamounts to the Major Seamount (Figure 12). The UU is thickest north and south the Cornaglia Seamount (Figure 12), where it locally reaches 0.4 to 0.45 stwtt thick (700 m to 790 m; Figure 14). The top of the UU deepens eastward across the southern part of the Cornaglia Terrace: it lies at 3.20 stwtt depth (~2450 m) at the eastern foot of the Quirra Seamounts (Figure 5, CDP 1640) and deepens at more than 4 stwtt depth (~3500 m) east and northeast of the Cornaglia Seamount (Figure 10).

5.4.1.4 *The UU in the East Sardinia Basin and the Cornaglia Terrace: comparison*

In the East-Sardinia Basin the UU is thin, in average less than 0.2 stwtt (*i.e.*, 350 m). On the Cornaglia Terrace, the thickness of the UU is comprised between 0.2 stwtt (*i.e.*, 350 m) and 0.45 stwtt (*i.e.*, 790 m). The UU is particularly thick in the southern part of the terrace, twice as much as in the East-Sardinia Basin (Figure 12).

In the East-Sardinia Basin (Figure 10), the top of the UU lies within a range from 2.5 to 3 stwtt (1800 m and 2500 m), excepted in its northernest part where the top of the UU is very shallow (less than 2 stwtt; 1300 m depth). On the Cornaglia Terrace, the top of the UU lies within a range from 2.9 to 4 stwtt (2100 m to 3100 m) depths in the northern terrace, and 3.20 to 4 stwtt (2400 to 3500 m) in the southern terrace. At the present day, the top of the UU lies significantly deeper on the Cornaglia Terrace than in the East-Sardinia Basin, by 300 m to 1000 m when comparing the highest and deepest values in both basins.

5.4.2 The Mobile Unit (MU)

The Mobile Unit corresponds to the "lower sequence" of Curzi et al. (1980) and the seismic facies n°6 and n°7 of Moussat (1983). The MU is located below the UU and shows a transparent seismic facies, although it locally displays internal low-amplitude reflectors (Figure 11, CDP 4300 to 4800). Because of its viscous behavior and weak mechanical strength, the MU locally deforms ductily (Figures 11 and 14) (Curzi et al., 1980; Moussat, 1983; Gaullier et al., 2014). The main salt basins correspond to the Cornaglia Terrace and the southernmost part of the East-Sardinia Basin (Figure 10). The north of the East-Sardinia Basin and the Cornaglia Terrace also display some smaller scale patches of MU. Everywhere the MU pinches out against the basement highs (*e.g.* Figure 13).

5.4.2.1 *The East-Sardinia Basin*

In the northern part of the East-Sardinia Basin, west of the northern tip of the Baronie Ridge, the MU is thin (<0.12 stwtt, ~270 m; Figure 7) and its top deepens from the edges of the

basin (2.75 stwtt depth, 2300 m; Figure 7, CDP 4200) toward the centre (3.11 stwtt depth, 2770 m; Figure 7, CDP 5450 and Figure 15). In the southern part of the East-Sardinia Basin, west of the Sardinia and Quirra Seamounts, the MU is thin as well (0.1-0.15 stwtt, *i.e.* ~225-340 m; Figure 5, CDP 2800 to 3800). The top of the MU deepens from the south toward the Gulf of Orosei (Figure 15): it lies at a depth of 2.68 stwtt (~ 2270 m) west of the Quirra seamounts and it is located at 3.35 stwtt depth (*i.e.* 2790 m) south of the Sardinia Seamounts. The MU pinches off against the structural highs at the rims the East-Sardinia Basin (Figures 5 and 7).

5.4.2.2 The Orosei Canyon area

North and northeast of the Sardinia Seamount, some small patches of MU are present in the Orosei Canyon area (Figure 15). The MU is thin, between 0.06 stwtt and 0.11 stwtt thick (~135 to 250 m). Its top is located between 2.92 stwtt (~ 2440 m) and 3.42 stwtt depth (~2770 m) (Figure 13). Along the southern flank of the Baronie Ridge we also observe two patches of MU in the channel of the Orosei Canyon (Figure 15).

5.4.2.3 The Cornaglia Terrace

In the northern part of the Cornaglia Terrace, at the eastern foot of the Baronie Ridge, the MU is confined within isolated basins (Figure 15). Eastward, between the Onifai Ridge and ODP Site 653, the MU is about 0.2 stwtt thick (~450m; Figure 2B). Its top deepens from the Baronie Ridge (3.25 stwtt depth, ~2625 m; Figure 15) towards the east (4.1 stwtt depth, ~3240 m; Figure 2B).

In the southern part of the Cornaglia Terrace the MU is thick, from 0.2 stwtt to more than 0.5 stwtt (> 1 km) in thickness. The top of the MU deepens from west to east in the southern part of the Cornaglia Terrace (Figure 15): it is located at 3.5 stwtt depth (~2930 m) east of the Sardinian Seamount and at 4.5 stwtt depth (~3315 m) east/southeast of the Cornaglia Terrace. Northeast of the Cornaglia Seamount the top of MU is even deeper, close to 4.6 stwtt depth

(~3980 m). Intense diapiric deformations in this part of the terrace (Figures 11 and 14) locally increased the initial thickness of the MU and disrupted the overlying brittle UU and PQ sedimentary cover.

5.4.2.4 The MU in the East Sardinia Basin and the Cornaglia Terrace: comparison

In the East-Sardinia Basin, the MU is thin, close to 0.1-0.15 stwtt thick (~225-340 m). The MU is significantly thicker on the Cornaglia Terrace, having thicknesses from 0.2 stwtt (~ 450 m) to 0,5 stwtt (~1100 m).

In the East-Sardinia Basin, the top of the MU lies at depths ranging between 2.68 stwtt and 3.35 stwtt (2270 m and 2800 m). On the Cornaglia Terrace, the top of the MU lies between 3.25 stwtt and 4.6 stwtt depths (2600 m and 4000 m) and it deepens from west to east (Figure 15). At the present-day, the top of the MU is then significantly deeper on the Cornaglia Terrace than in the East-Sardinia Basin, from 330 m to 1200 m when comparing the highest and deepest values in both basins.

5.5 Other MSC markers

Along the Eastern Sardinian margin, the Lower Unit (LU) visible beneath the MU in the Gulf of Lions (Lofi et al., 2005) could not be evidenced. Curzi et al. (1980) suggested the presence of a lower evaporitic unit below the MU, but where the base of the MU is visible (Figure 8), we can not observe clear bedded unit or any seismic signature related to evaporites below the MU. Because of the lack of seismic penetration through the salt, we then can not confirm or contradict the hypothesis from Curzi et al. (1980).

The Complex Unit (CU), which is widely present in other Mediterranean basins (Lofi et al., 2005; Maillard et al., 2006; Lofi et al., 2011a; Obone-Zué-Obame et al., 2011), is visible only very locally in our study area, along the flank of some structural highs (Figure 10): on the western flank of the Quirra Seamounts (Figure 5), nearby the Cornaglia Seamount (Figure 11), or at the southeastern foot of the Baronie Ridge (Figure 16). Where observed, the CU

consists of a chaotic facies having discontinuous, high-amplitude internal reflectors. It shows a lateral interfingered transition with the MSC units UU and MU (Figure 16).

6 DISCUSSION

Lofi et al. (2011b) suggested that the MSC surfaces and units can be used as markers for paleogeographic reconstructions. In the deepest parts of the Mediterranean basins, the MU is thought to have accumulated by evaporative drawdown (Ryan and Cita, 1978; Lofi et al., 2011b; Ryan, 2011), while the UU would subsequently have aggraded under lowered sea-level conditions (Maillard and Mauffret, 2006; Lofi et al., 2011b). The MES is then interpreted as a polygenic surface of mainly sub-aerial origin (Ryan, 1973; Stampfli and Höcker, 1989; Lofi et al., 2011b). Lofi et al. (2011b) also suggested that the onlap points of the UU could be used to approximately locate the position of the paleo-coastline at a basin scale, during the drawdown phase. The onlap point of the UU could thus be used for quantitative paleo-reconstructions. Therefore, in our study, we consider that the MSC units accumulated in the paelo-bathymetric lows, whereas areas located landward of the pinch-out of the UU corresponded to palaeo-bathymetric or topographic highs that underwent sub-aerial erosion during the MSC. Accordingly, we used the MSC markers of the Eastern Sardinia margin as tools to understand the paleomorphology of the margin during the MSC.

6.1 Paleogeography of the Eastern Sardinia margin during the MSC

6.1.1 The MSC units as markers of Messinian bathymetric lows

The present-day Eastern Sardinian margin displays two main MSC basins: the East-Sardinia Basin and the Cornaglia Terrace (Figure 10), the second deeper than the first. The presence of the MSC units in these basins means that they were already structured during the MSC, forming bathymetric lows which allowed for the deposition of the MU and UU. The MSC units logically accumulated in grabens previously formed during the rifting, and that offered accommodation (Figure 10). This is consistent with the fan-shaped reflectors (in blue on

Figures 2A, 4 and 5) and their associated normal faults that we observe below the MSC markers and that we interpret as being the syn-rift markers, of a probable Tortonian age, *c.* 11 Ma, and earlier (Langhian? *c.*15 Ma; Carminati et al., 2012).

6.1.2 The Margin Erosion Surface (MES) as a marker of Messinian topographic highs

Along the Eastern Sardinian margin, the MES extends on the uppermost continental slope and at the top of isolated structural highs visible in the present-day bathymetry (Figure 10). On some local highs, an erosion surface geometrically disconnected from the MSC units is observed (Figure 11). We assume that this erosion surface corresponds to the MES overlain by PQ deposits. It implies that the structural highs were already forming topographic highs during the MSC, elevated high enought to prevent deposition of the MU and UU accumulated in topographic lows.

On the continental slope offshore the Orosei Gulf the MES forms a network of palaeo-valleys that deeply incise through the pre-MSC deposits (Figure 4, 6 and 10). These paleo-valleys likely formed in a subaerial environment during the MSC drawdown phase (Chumakov, 1973; Clauzon, 1973; Lofi et al., 2011b) and a possible scenario is that this network represents an evidence of extensive subaerial exposure of the margin while the base-level was drastically lowered. The MES is steadily observed on the structural highs, while in the basins the pinch-out of the MU is located deeper than the MES (Figures 10 and 17). It suggests that the base-level was substantially lowered during the accumulation of MU, as already proposed in former studies (Rouchy and Caruso, 2006; Lofi et al., 2011a, b), while the edges of the basins where under subaerial exposure setting. This is also supported by the local presence of the CU, generated during the erosion, which is interfingered with the MU (Figures 5, 11 and 16) or directly incorporated within the mobile salt layer, resulting in a not transparent seismic facies of the MU (Figures 7 and 11). In several places (*e.g.* Figures 7 and 8), the BS at the base of the MU switches to the BES toward the edge of the salt layer and beneath the onlaps

of the UU; this supports the idea that MU accumulated in areas deep enough to prevent subaerial erosion below the salt and then that the aggradation of UU occurred on an eroded surface (the BES) formerly under subaerial-exposure. Meanwhile, the upper parts of the slopes were still under erosion, as shown by the interfingering between the UU and the CU (Figures 5, 11 and 16) and by the incorporation of clastic material within the UU (Figure 13). If we support the MES mainly results from subaerial erosional processes, particularly upslope were its morphology is the roughest (Figure 4), we do not exclude the possibility of subaqueous reworking downslope where the MES is smoother (Figure 6) possibly as the result of wave ravidement during the refilling phase of the basin (Bache et al., 2009; Garcia et al., 2011). The local shaping of the MES by gravity flows is also not excluded. The generation of the MES under subaqueous processes only (Roveri et al., 2016) remains however in our view difficult to reconcile with the deeply incising morphology of this surface on the upper slope, its widespread extension, and the aggrading geometry of the UU in the topographic lows.

As a consequence of the above reasoning, and in concordance with Lofi et al. (2011), we interpret the MES as being a diachronic and polygenic surface whose age covers the period of time between the first sea-level drawdown and the complete reflooding of the basin when the erosion stopped and the first Pliocene deposits sealed the erosion surface.

6.1.3 The Eastern Sardinia margin: a margin already segmented at the time of the MSC

In the Western Mediterranean basins, the MES has locally been evidenced on isolated structural highs that were formed before the MSC, along the West- and East-Corsica margins (Guennoc et al., 2011; Cornamusini and Pascucci, 2014; Cocchi et al., 2015; Thinon et al., 2016), on the Valencia Seamount (Mitchell and Lofi, 2008) or on the Balearic promontory (Driussi et al., 2015). Another example of isolated structural high with the MES ontop also exists in the Eastern Mediterranean Sea, with the Eratosthenes Seamount that formed before

the MSC and was eroded during the crisis, while the MSC evaporites precipitated in the surrounding deeper basin (Major and Ryan, 1999; Loncke et al., 2006; Loncke et al., 2010). Because the present-day distribution of the MSC seismic markers in the Western Tyrrhenian Basin evidences the presence of MSC units in the present-day bathymetric lows and of the MES on the present-day topographic highs (Figure 10), we then conclude that the present-day Eastern Sardinia margin was already segmented with the same highs and lows during the MSC. Thus, the paleogeography of the margin included several small islands (for example the "Baronie Island" and the "Onifai Island"), subjected to subaerial erosion by the time of the MSC drawdown phase, whereas the MSC units were deposited in the basins around these islands.

6.2 The Western Tyrrhenian Basin: Which status during the Messinian Salinity Crisis?

6.2.1 Timing of rifting along the Eastern Sardinia margin

It is very clear that the syn-rift markers (blue horizons on figures 4 and 5) are pre-MSC in age on the flanks of the East-Sardinia Basin and on the western Cornaglia Terrace. Firstly because they are buried below pre-MSC post-rift deposits (pink reflectors of Tortonian age). Secondly, because the faults associated to the rifting do not affect this pre-MSC post-rift unit, or the MSC markers above (Figures 4 and 5). In our opinion, these geometries support the interpretation that the rifting ended before the MSC in this sector of the Sardinia margin. These observations are also consistent with the present-day distribution of the MSC seismic markers (Figure 10 and 17) that shows the Eastern Sardinian margin was, as a result of the rifting, already segmented in horsts and grabens before the MSC.

Further east, at ODP Sites 654 and 653 (Figure 2), the lithostratigraphic units VI, V and IV, all pre-MSC in age, evidence a clear transgressive sequence related to the rifting of the margin (Kastens et al., 1988; Mascle and Réhault, 1990). The Plio-Quaternary ooze and the

MSC evaporites (Lithostratigraphic units I and II, Figure 2) have been interpreted as being post-rift in age (Kastens et al., 1988; Mascle and Réhault, 1990), which is in good agreement with the pre-MSC age of the syn-rift markers on the upper continental slope (Figures 4 and 5). An ambiguous interpretation concerns the lithostratigraphic unit III drilled at ODP site 654 (see section 2.3) and considered as being syn-rift on the base of micro-faults observed within the unit (Kastens et al., 1988). Lithostratigraphic unit III is not included in the syn-rift sequence in later publications (Kastens, 1992), suggesting an incertitude regarding the syn-rift character of this unit. This incertitude makes sense as the unit has been deposited during the first stages of the MSC (Kastens et al., 1988; Kastens, 1992; Roveri et al., 2014a) thus recording the initiation of strong palaeo-environmental changes in settings of deposition. Moreover, lithostratigraphic unit III being 36 m thick (Kastens et al., 1988; Kastens, 1992), the seismic resolution is too low to allow for checking if this unit belongs or not to the syn-rift sedimentary fan observed on the seismic data (Figure 2A).

We interpret this lithostratigraphic unit III at site ODP 654 as being post-rift, in agreement with the observations further west. In this scenario, the micro-faults observed within cores (Kastens et al., 1988) could be related to other process, such as the development of polygonal faults, a common feature of claystones (Cartwright et al., 2003) and post-rift sequences in rifted basins (Cartwright, 1994). A conclusion of this reasonement is that in the East-Sardinia Basin and on the Cornaglia Terrace, the rifting ended before the MSC.

This conclusion differs from the one of Sartori *et al.* (2001; 2004) who considered that in the East-Sardinia Basin and on the Cornaglia Terrace, the "Tortonian *p.p.* to Pliocene *p.p.* series" are syn-rift, thus including the MSC series. On the Cornaglia Terrace, our data locally show fan-shaped strata in the UU (Figure 11, CDP 2200 to 3000; Figure 14, CDP 3000 to 3450). However, as demonstrated by Gaullier et al. (2014), we interpret these geometries as related to salt tectonics and diapirism of the underlying MU, rather than to rifting. We thus do not

observe syn-rift MSC deposits or evidence of rifting during the MSC or the Pliocene. One may argue that even if crustal faults were active during the accumulation of the MU, their movement would be masked by the ductile flow of the overlying mobile salt, which is particularly thick where the pre-MSC rifting had generated bathymetric lows. However, in areas where the MU is thin or absent, our data do not show any syn-rift geometries in the UU (Figures 2, 5 and 6).

6.2.2 When the MSC meets geodynamics

6.2.2.1 Discussion on the paleo-depth of the Eastern Sardinia margin at the end of the pre-MSC rifting.

Figure 17 shows two dip sections based on METYSS data and summarizing the present-day organisation of the MSC seismic markers across the Eastern Sardinian margin. The sections are located on the Figure 1, respectively in the Orosei Canyon area (Figure 17A) and in the southern East-Sardinia Basin and Cornaglia Terrace (Figure 17B). The sections allow comparing the present-day organisation of the MSC seismic markers in the Western Tyrrhenian Basin with the one on the Western Sardinia (Figure 18A) and the Provencal margins (Figure 18B) on which the MSC markers are also post-rift in age (Thomas et al., 1988; Obone Zue Obame et al., 2011; Sage et al., 2011; Geletti et al., 2014). These margins belong to the Algero-Provençal Basin, which is regarded as an offshore *deep* MSC basin (Figure 3; CIESM, 2008), because the rifting was finished before the MSC (Gueguen et al., 1998; Jolivet and Faccenna, 2000; Jolivet et al., 2006). This deep basin accumulated thick deposits during the MSC (Montadert et al., 1970; CIESM, 2008; Lofi et al., 2011a, b): the "Messinian trilogy". The MSC sedimentary records in both the Algero-Provençal and Western Tyrrhenian basins present strong similarities (Figures 17 and 18): in each basin the MSC deposits include a thick salt layer, MU, overlained by an upper unit, UU, very similar in term of thicknesses (when non deformed by salt tectonics, UU is brodaly ranging from 0 to

0.25-0.3 stwtt thick in both basins). The present-day pinch-out the UU on the Eastern Sardinia, Western Sardinia and Western Provençal margins also occurs in the same range of depth (Figures 17 and 18). Based on these similarities and according to the present-day definition of the status of the MSC basins (see section 3), we conclude that at least some parts of the Tyrrhenian Basin (the Cornaglia Terrace) were forming *deep* basins at the time of the MSC. This is related to the fact that the rifting of the margin ended before the start of the crisis and the MSC occurred above thinned continental crust that was likely very deep, with water depth that probably reached 1000 m and beyond. This is consistent with the Tortonian to Early Messinian age of the pre-MSC listhostratigraphic unit IV recorded at ODP site 654A, which is made of nanofossil chalk representative of environment of "several hundreds meters water depth" (Kastens, 1992) that deposited a few million years before the onset of the crisis.

The significant depth of the Western Tyrrhenian Basin during the MSC can also be estimated thanks to a comparison between the present-day depth of the MSC markers and the amount of post-MSC subsidence proposed by Curzi et al. (1980) for the Eastern Sardinian margin.

At the present-day, the top of the MU is located between 2.68 stwtt for the shallowest and 4.5 stwtt for the deepest (Figure 15), which correspond respectively to 2270 m and 3650 m below the sea level. In the case where the East Sardinia margin underwent 1000 or 1500 m of post-MSC subsidence, as proposed by Curzi et al. (1980), the top of the salt was thus possibly located between, respectively, 1270 and 2650 m or 770m and 2150 m below the sea level. Except for the value of 770 m, these depths clearly correspond to the range of the deep (> 1000 m) MSC basins (Figure 3; CIESM, 2008). Knowing that in the Western Tyrrhenian Basin the salt is several hundreds meters thick (locally more than 1 km), the palaeo-seafloor before the accumulation of the MU was then even deeper.

The *deep* status that we propose for the Western Tyrrhenian Basin is in contradiction with the *intermediate* status sugested by Roveri *et al.* (2014a). Based on the studies of evaporite facies in cores (Lugli et al., 2015) and Strontium data (Roveri et al., 2014a), the UU at Site 654 are thought to be the equivalent in term of depositional environment and timing of the MSC Upper unit in Sicily, although emplaced at slightly deeper water depth. Extrapolating this interpretation to the entire Tyrrhenian Basin, Roveri et al. (2014a) thus consider the Tyrrhenian as an intermediate basin during the MSC. In our study however, the seismic data clearly show that the MSC record at site 654 is incomplete as the MU is missing and only part of the UU is present, as shown by the the internal reflectors of UU onlapping the pre-MSC topography (Fig. 2A). For this reason, if deposits at Site 654 can be considered as emplaced in intermediate basin, they are not representative of the records in the deepest part of the basin where both the MU and UU are present (Figure 10). The lack of any indication of shallow-water settings and of desiccation in the cores at Site 654 (Lugli et al., 2015) is not incompatible the emplacement of the UU following a pronounced sea-level fall and infilling the basin under relative shallow water depth (not necessariliy below fairweather base level).

6.2.2.2 Bathymetric paleo-relief of the Eastern Sardinia margin at the end of the pre-MSC rifting

Across the Eastern Sardinian margin, the East-Sardinia Basin and the Cornaglia Terrace show a present-day stair-stepped geometry (Figure 17) inherited from the rifting phase. Both in the East-Sardinia Basin and on the Cornaglia Terrace, the MSC seismic units show the same seismic facies and the same organisation (Figure 17), *i.e.* with the MU underlying the UU. The current locations of our seismic lines however do not allow us to clearly image the lateral continuity of the MSC units between the two basins. Previous studies (Curzi et al., 1980; Moussat, 1983) mapped out paleo-connections between the two basins during the MSC (Figure 10, *e.g.* around the Sardinia Seamount), suggesting that the UU can be traced

continuously from the East-Sardinia Basin to the Cornaglia Terrace. This lateral connexion suggests that the UU precipitated coevally in the Western Tyrrhenian sub-basins. However, the MSC series are clearly thicker on the Cornaglia Terrace compared to the East-Sardinia Basin (Figure 17) and the tops of the UU and the MU on the Cornaglia Terrace are currently lying 300 m to 1200 m deeper than in the East-Sardinian Basin. These differences in depth and thicknesses can be explained in different ways discussed hereafter.

The difference of thickness of the MSC units in each basin may firstly partly result from the pre-existing MSC paleo-topography coupled with the base-level changes during the crisis. Indeed, the emplacement of the MU by evaporative drawdown (Ryan and Cita, 1978; Lofi et al., 2011b; Ryan, 2011) could explain why the salt is thicker in the Cornaglia Terrace, which was deeper compared to the East-Sardinia Basin and offered more accommodation. In this model, the precipitation of the halite in thicknesses is inversely proportional to elevation above the basin floor and MU deposition is possibly completed under shallow water conditions, as supported by the presence of the MES on the surrounding structural highs (Figure 10). For this reason it is not excluded that the top of the MU in the East-Sardinia Basin was temporarly submitted to sub-aerial exposure and dessication while the deposition of MU was completed at depth, on the Cornaglia Terrace. Following the emplacement of MU, the UU possibly deposited under relative shallow water depth (Lofi et al., 2011b), filling topographic lows, starting in the deepest parts of the margin (*i.e.* the Cornaglia Terrace). As the relative base-level rose, the UU progressively filled more shallow parts (*i.e.* the East-Sardinia Basin), onlapping on the pre-MSC basement at the rim of the basins. This scenario is supported by the aggrading character of the UU over the BES ontop of the pre-MSC basement (*e.g.* Figures 8, 9, 11). This reasonment would thus explain why the UU is thicker in the deeper setting (Cornaglia Terrace) than in the shallower settings (East-Sardinia Basin) and is consistent with a stair-stepped geometry of the margin (Figure 17) at the start of the

MSC. The importance of pre-MSC paleo-bathymetries in the lateral variability in thickness of the UU has already been highlighted by Maillard et al. (2006) in the Valencia Basin, which, due to its shallower setting at the start of the MSC, contains thinner UU compared to the deeper Liguro-Provençal Basin.

The present-day difference in depth of the onlaps of the UU, lying 300 m to 1000 m deeper in the Cornaglia Basin compared to the East-Sardinian Basin (Figure 17) need to be explained. In the Western Mediterranean Basin, it has been suggested that the pinch-out of the UU marks the location of one paleo-coastline before the achievement of the MSC and thus reflects one given paelo-depth at the scale of one basin (Lofi et al., 2011b). Following this reasoning, the difference in the present-day depth of the pinch-out of the UU between the Cornaglia Basin compared to the East-Sardinian Basin would reflects a different amount of post-Messinian vertical deformation (subsidence, compaction, uplift, differencial post-MSC thermal subsidence), undergone by each margin and basin during their post-rift evolution. Indeed, Gaullier et al. (2014) demonstrated that some of the major faults in the north of the margin have been significantly reactivated during the post-rift period, up to late Quaternary time. Curzi et al. (1980) also suggested that strong post-MSC vertical motions could have caused the offset of the MSC units across the margin. However the top of the UU lies up to 1000 m deeper in the Cornaglia Terrace than in the East-Sardinia Basin, thus requesting a strong and localized thermal subsidence in the Cornaglia terrace. Although post-rift vertical movements locally exist on the margin and are attested by the vertical offset the MSC markers (Figures 7 and 9), we do not observe on the METYSS data any evidences for crustal post-MSC motions that would be strong enough to accomodate such a difference of depth between the East-Sardinia Basin and the Cornaglia Terrace. We do not observe neither any post-MSC major fault active at the transition between the East-Sardinia Basin and the Cornaglia Terrace (Figure 5) and the top of the UU, as well as the PQ reflectors, overall

remain relatively flat and horizontal across the margin (Figure 17). A possible alternative explanation inferred by the prestructuration of the Sardinian margin would be that the UU was deposited below different water depths in the East-Sardinia and the Cornaglia Terrace, implying that both basins were possibly disconnected. In such a case, the different onlaps of the UU (Figure 17) could not be used as a tool to quantify the post-MSC deformation across the Eastern Sardinia margin. The emplacement of the UU at various water depth is however difficult to reconciliate with both the agrading geometry of the UU and its potential continuity (Curzi et al., 1980; Moussat, 1983) from the East-Sardinia Basin to the Cornaglia Terrace (Figure 10). However, this interpretation cannot be definitely rulled out and further studies are required especially over the complex transitional domain between the two basins. We support that the present-day differences in depth of the onlaps of the UU across the margin are partly inherited from the deposition process of the UU. Thus it would be hazardous to use these onlaps to quantify the post-MSC subsidence of the sub-basins across the margin without the acquisition of additional seismic lines, both oriented East-West and North-South. Such additional data would allow for investigate the lateral extension of the UU from the East-Sardinia Basin to the Cornaglia Terrace, as well as to document the longitudinal variations of depth of the seismic markers in each basin. This would eventually allow for backstripping restoration to understand the post-MSC geodynamic evolution of the Eastern Sardinian margin.

7 CONCLUSION

In this study we revisited the MSC seismic markers across the Eastern Sardinian margin from the interpretation of the METYSS seismic dataset. Based on the distribution and depths maps of these markers we have shown that the MSC units have precipitated in palaeo-bathymetric lows, whereas the MES develloped on the basement highs. We also demonstrate that across the margin the syn-rift deposits are pre-MSC in age (Tortonian or older), because they are

located below the MSC seismic markers, which do not show any evidence for syn-rift deformation. The MSC seismic markers thus provide powerfull time-markers to bracket the age of the rifting in the Western Tyrrhenian Basin. These observations reveal that the Eastern Sardinian margin was already segmented in horsts and grabens during the MSC and imply that the rifting of the East-Sardinia Basin and the Cornaglia Terrace ended before the MSC. As a consequence we conclude that the East-Sardinian Basin and the Cornaglia Terrace already structured in a stair-stepped geometry before the MSC, which is consistent with the absence of strong post-MSC fault crustal activity at the transition between both basins. Then this pre-existing topography combined with base level changes during the deposition of the MU and UU can explain the present-day differences of thickness of the MSC units that we evidence between the East-Sardinian Basin and the Cornaglia Terrace. The present-day difference in elevation between these units can possibly be explained by differential post-Messinian vertical deformation (compaction, differencial post-MSC thermal subsidence). However the deposition of the MSC units below different water depth in both basins cannot be ruled out, with the consequence that, for now, we cannot confidently use the present-day onlaps of the UU as marker to quantify the post-rift subsidence of the Eastern Sardinia margin. Locally, the MSC series show some signs of synsedimentary deformation, but this can be attributed to thin-skinned salt tectonics. An implication is that most of the Western Tyrrhenian Basin was already a deep basin with significant water depth (1000 m and more) when the MSC started. This is also supported by the comparison of the MSC records with known deep MSC basin, for instance the Algero-Provencal Basin.

ACKNOWLEDGMENTS

The “METYSS” cruises were supported by the French “ACTIONS MARGES” and “ACTION COORDONNEE” INSU programs. We warmly thank the Captains of the R/V « Téthys II » (INSU/CNRS), Rémy Lafond and Joël Le Guennec and their crews for data

acquisition during “METYSS 1” and “METYSS 3” cruises. William B. F. Ryan and two anonymous reviewers provided constructive reviews that improved this work and are therefore deeply acknowledged.

REFERENCES CITED

1) Bache, F., Olivet, J.-L., Gorini, C., Rabineau, M., Baztan, J., Aslanian, D. and Suc, J.P., 2009. Messinian erosional and salinity crises: View from the Provence Basin (Gulf of Lions, Western Mediterranean). Earth and Planetary Science Letters, 286, 1-2, 139-157, doi: 10.1016/j.epsl.2009.06.021.

2) Bertoni, C., Cartwright, J.A., 2006. Controls on the basinwide architecture of late Miocene (Messinian) evaporites on the Levant margin (Eastern Mediterranean). Sedimentary Geology, 188-189, 93-114, doi: 10.1016/j.sedgeo.2006.03.019.

3) Cameselle, A.L., and Urgeles, R., 2017. Large-scale margin collapse during Messinian early sea-level drawdown: the SW Valencia trough, NW Mediterranean. Basin Research (2017), 29 (Suppl. 1), 576–595, doi: 10.1111/bre.12170

4) Carminati, E., Lustrino M., Doglioni, C., 2012. Geodynamic evolution of the central and Western Mediterranean: Tectonics vs. igneous petrology constraints. Tectonophysics, vol. 579, p. 173–192, doi: 10.1016/j.tecto.2012.01.026.

5) Carrara, G., 2002. Evoluzione cinematica neogenica del margine occidentale del bacino tirrenico. Doctoral dissertation, Dipartimento di Scienze delle Terra dell'Univerità di Parma. 160p.

6) Cartwright, J., 1994. Episodic basin-wide hydrofracturing of overpressured Early Cenozoic mudrock sequences in the North Sea Basin. Marine and Petroleum Geology, 1994, Volume 11, Number 5, doi: 10.1016/0264-8172(94)90070-1.

7) Cartwright, J., James, D. and Boston, A.L., 2003. The genesis of polygonal fault systems: a review. In: Van Rensbergen P., Hillis R.R., Maltan A.J., and Morley C.K., (eds) 2003.

Subsurface sediment mobilization. Geological Society of London, Special publication, 216, 223-243, doi: 10.1144/GSL.SP.2003.216.01.15.

8) Caruso, A., Pierre, C., Blanc-Valleron, M.-M., Rouchy, J.M., 2015. Carbonate deposition and diagenesis in evaporitic environments: The evaporative and sulphur-bearing limestones during the settlement of the Messinian Salinity Crisis in Sicily and Calabria. Palaeogeography, Palaeoclimatology, Palaeoecology, 429, 136–162, doi: 10.1016/j.palaeo.2015.03.035.

9) Chumakov, I.S., 1973. Geological history of the Mediterranean at the end of the Miocene, and the beginning of the Pliocene according to new data. In: W.B.F. Ryan, K.J. Hsü et al., Initial Reports of the Deep Sea Drilling Project, 13(2). U.S. Government Printing Office, Washington, D.C., pp.1241-1242.

10) CIESM (Anton, J., Çagatay, M.N., De Lange, G., Flecker, R., Gaullier, V., Gunde-Cimerman, N., Hübscher, C., Krijgsman, W., Lambregts, P., Lofi, J., Lugli, S., Manzi, V., McGenity, T.J., Roveri, M., Sierro, F.J. and Suc, J.-P.), 2008. Executive summary. In: The Messinian Salinity Crisis From Mega-Deposits to Microbiology – A Consensus Report (Ed. by F. Briand), CIESM Workshop Monographs, 33, 7–28.

11) Cita, M.B., Santambrogio, S., Melillo, B., Rogate, F, 1990. Messinian paleoenvironments: new evidence from the Tyrrhenian Sea (ODP LEG 107). In: Kastens, K. A., Mascle, J., et al., 1990 Proceedings of the Ocean Drilling Program, Scientific Results, Vol. 107.

12) Clauzon G., 1973. The eustatic hypothesis and the pre-Pliocene cutting of the Rhône valley. In: Ryan, W.B.F. & Hsu, K.J., Eds., Initial Report of the Deep Sea Drilling Project, 1251-1256.

13) Clauzon, G., Suc, J.-P., Gautier, F., Berger, A. and Loutre, M.-F., 1996. Alternate interpretation of the Messinian Salinity Crisis: controversy resolved? Geology, 24 (4), 363–366, doi: 10.1130/0091-7613-31.1.e23.

14) Cobbold, P.R., Rosselo, E.A., and Vendeville, B., 1989. Some experiments on interacting sedimentation and deformation above salt horizons. Bulletin de la Societé Géologique de France, 5 (3): 453–460.

15) Cocchi, L., Masetti, G., Muccini, F. and Carmisciano, C., 2015. Geophysical Mapping of Vercelli Seamount: Implications for Miocene Evolution of the Tyrrhenian Back Arc Basin. Geoscience Frontiers, Volume 7, Issue 5, September 2016, Pages 835–849, doi: 10.1016/j.gsf.2015.06.006.

16) Cornamusini, G., and Pascucci, V., 2014. Sedimentation in the Northern Apennines-Corsica tectonic knot (Northern Tyrrhenian Sea, Central Mediterranean): offshore drilling data from the Elba-Pianosa Ridge. International Journal of Earth Sciences 103, 2014, 821–842, doi: 10.1007/s00531-014-0998-5.

17) Curzi, P., Fabbri, A., Nanni, T., 1980. The Messinian evaporitic event in the Sardinian basin area (Tyrrhenian Sea). Marine Geology, 34, 157-170, doi: 10.1016/0025-3227(80)90070-5.

18) Dela Pierre, F., Bernardi, E., Cavagna, S., Clari, P., Gennari, R., Irace, A., Lozar, F., Lugli, S., Manzi, V., Natalicchio, M., Roveri, M., Violanti, D., 2011. The record of the Messinian salinity crisis in the Tertiary Piedmont Basin (NW Italy): the Alba section revisited. Palaeogeography, Palaeoclimatology, Palaeoecology, 310, 238–255, doi: 10.1016/j.palaeo.2011.07.017.

19) Dela Pierre, F., Natalicchio M., Ferrando S., Giustetto R., Birgel D., Carnevale G., Gier S., Lozar F., Marabello D., Peckmann J., 2015. Are the large filamentous microfossils

preserved in Messinian gypsum colorless sulfide-oxidizing bacteria? Geology (2015), 43 (10): 855-858, DOI: https://doi.org/10.1130/G37018.1.

20) Dewey, J.F., Helman, M.L., Turco, A., Hutton, D.H.W, Knott, S.D., 1989. Kinematics of the western Mediterranean. In: Coward, M. P., Dietrich, D., and Park, R.G., (eds), Alpine Tectonics, Geological Society Special Publication, No. 45, pp. 265-283, doi: 10.1144/GSL.SP.1989.045.01.15.

21) Doglioni, C., Innocenti, F., Morellato, C., Procaccianti, D., and Scrocca, D., 2004. On the Tyrrhenian Sea opening. Memorie Descrittive della Carta Geologica d'Italia, 64, 147-164.

22) Driussi, O., Maillard, A., Ochoa, D., Lofi, J., Chanier, F., Gaullier, V., Briais, A., Sage, F, Sierro, F., Garcia, M., 2015. Messinian Salinity Crisis deposits widespread over the Balearic Promontory: Insights from new high-resolution seismic data. Marine and Petroleum Geology, 66, 41-54, doi: 10.1016/j.marpetgeo.2014.09.008.

23) García, M., Maillard, A., Aslanian, D., Rabineau, M., Alonso, B., Gorini, C., Estrada, F., 2011. The Catalan margin during the Messinian Salinity Crisis: Physiography, morphology and sedimentary record. Marine Geology, Volume 284, (1-4), 158-174, 2011, doi : 10.1016/j.margeo.2011.03.017.

24) Gaullier, V., Chanier, F., Lymer, G., Vendeville, B., Maillard, A., Thinon, I., Lofi, J., Sage, F., Loncke, L., 2014. Salt tectonics and crustal tectonics along the Eastern Sardinian margin, Western Tyrrhenian: New insights from the « METYSS 1 » cruise. Tectonophysics, http://dx.doi.org/10.1016/j.tecto.2013.12.015.

25) Geletti, R., Zgur, F., Del Ben, A., Buriola, F., Fais, S., Fedi, M., Forte, E., Mocknik, A., Paoletti, V., Pipan, M., Ramella, R., Romeo, R., Romi, A., 2014. The Messinian Salinity Crisis: New seismic evidence in the West-Sardinian Margin and Eastern Sardo-

Provençal basin (West Mediterranean Sea). Marine Geology, Volume 351, 76-90, doi: 10.1016/j.margeo.2014.03.019.

26) Gueguen, E., Doglioni, C., Fernandez, M., 1998. On the post-25 Ma geodynamic evolution of the Western Mediterranean. Tectonophysics, 298, 259–269, doi: 10.1016/S0040-1951(98)00189-9.

27) Guennoc, P., Gorini, C., and Mauffret, A., 2000. Histoire géologique du Golfe du Lion et cartographie du rift Oligo-Aquitanien et de la surface messinienne. Géologie de la France, 3, 67-97.

28) Guennoc, P., Réhault, J.P., Thinon, I., 2011. Western Corsica, in: Lofi, J., Deverchère, J., Gaullier, V., Gillet, H., Gorini, C., Guennoc, P., Loncke, L., Maillard, A., Sage, F. and Thinon, I., 2011, Seismic atlas of the "Messinian Salinity Crisis" markers in the Mediterranean and Black Seas: Commission for the Geological Map of the World (CGMW) / Mémoires de la Société Géologique de France, n.s., 179, 72 pp., 1 CD.

29) Hsü, K. J., Cita, M. B., and Ryan, W. B. F., 1973. The origin of the Mediterranean evaporates. In: Ryan W.B.F. et al., Eds., Initial reports of the deep sea drilling project. Washington, U.S. Government Printing Office, 1203-1231.

30) Jolivet, L., and Faccenna, C., 2000. Mediterranean extension and the Africa-Eurasia collision. Tectonics, 19, 6, 1095-1106, doi: 10.1029/2000TC900018.

31) Jolivet, L., Augier, R., Robin, C., Suc, J.-P., Rouchy, J.-M., 2006. Lithospheric-scale geodynamic context of the Messinian Salinity Crisis. Sedimentary Geology, 188-189, 9-33, 10.1016/j.sedgeo.2006.02.004.

32) Kastens, K.A., Mascle, J., Auroux, C., Bonatti, E., Broglia, C., Channell, J., Curzi, P., Emeis, K-C., Glaçon, G., Hasegawa, S., Hieke, W., Mascle, G., Mccoy, F., Mckenzie, J., Mendelson, J., Müller, C., Réhault, J-P., Robertson, A., Sartori, R., Sprovieri, R., and

Torii, M., 1988. ODP Leg 107 in the Tyrrhenian Sea: Insights into passive margin and back-arc basin evolution: Geological Society of America Bulletin, 100, 1140–1156.

33) Kastens, 1992. Did glacio-eustatic sea level drop trigger the Messinian Salinity Crisis? New evidence from Ocean Drilling Programm site 654 in the Tyrrhenian Sea; Paleoceanography, Vol. 7, No.3, Pages 333-356, June 1992.

34) Krijgsman, W., Hilgen, F.J., Raffi, I. & Sierro, F.J., 1999a. Chronology, causes and progression of the Messinian Salinity Crisis. Nature, 400, 652-654, doi: 10.1038/23231.

35) Krijgsman, W., Langereis, C.G., Zachariasse, W.J., Boccaletti, M., Moratti, G., Gelati, R., Iaccarino, S., Papani, G., Villa, G., 1999b. Late Neogene evolution of the Taza-Guercif Basin (Riftian Corridor, Morocco) and implications for the Messinian Salinity Crisis. Marine Geology 153, 147– 160.

36) Lofi, J., Rabineau, M., Gorini, C., Berné, S., Clauzon, G., DeClarens, P., Dos Reis, T., Mountain, G.S., Ryan, W.B.F., Steckler, M. and Fouchet, C., 2003. Plio-Quaternary prograding clinoform wedges of the Western Gulf of Lions continental margin (NW Mediterranean) after the Messinian Salinity Crisis. Marine Geology 198, 289–317, doi: 10.1016/S0025-3227(03)00120-8.

37) Lofi, J., Gorini, C., Berne, S., Clauzon, G., Dos Reis, A. T., Ryan, W. B. F. and Steckler, M. S., 2005. Erosional processes and paleo-environmental changes in the Western Gulf of Lions (SW France) during the Messinian Salinity Crisis. Marine Geology, 217, 1-30, doi: 10.1016/j.margeo.2005.02.014.

38) Lofi, J., Deverchère, J., Gaullier, V., Gillet, H., Gorini, C., Guennoc, P., Loncke, L., Maillard, A., Sage, F. and Thinon, I., 2011a. Seismic atlas of the "Messinian Salinity Crisis" markers in the Mediterranean and Black Seas: Commission for the Geological Map of the World (CGMW) / Mémoires de la Société Géologique de France, n.s., 179, 72 pp., 1 CD.

39) Lofi, J., Sage, F., Déverchère, J., Loncke, L., Maillard, A., Gaullier, V., Thinon, I., Gillet, H., Guennoc, P., Gorini, C., 2011b. Refining our knowledge of the Messinian Salinity Crisis records in the offshore domain through multi-site seismic analysis: Special Issue «Miocene-Pliocene geodynamics and paleogeography in the Mediterranean region: eustasy-tectonics interference». Bulletin de la Société géologique de France, 182 (2), 163-180.

40) Loget, N., and Van Den Driessche, J., 2006. On the origin of the strait of Gibraltar. Sedimentary Geology, 188-189, 341-356, doi: 10.1016/j.sedgeo.2006.03.012.

41) Loncke, L., Gaullier, V., Mascle, J., Vendeville, B.C., and Camera, L., 2006. Nile deep-sea fan: an example of interacting sedimentation, salt tectonics, and inherited subsalt paleotopographic features. Marine and Petroleum Geology, 23, 297-315, doi: 10.1016/j.marpetgeo.2006.01.001.

42) Loncke, L., Vendeville, B. C., Gaullier, V., and Mascle, J., 2010. Contributions of tectonic and gravity-driven processes on the structural pattern in the Eastern Nile deep-sea fan: Insights from physical experiments. Basin Research, 22, 765-782, doi: 10.1111/j.1365-2117.2009.00436.x.

43) Lugli, S., Manzi, V., Roveri M., Schreiber C. B., 2015. The deep record of the Messinian salinity crisis: Evidence of a non-desiccated Mediterranean Sea, Palaeogeography, Palaeoclimatology, Palaeoecology 433, 201–218, http://dx.doi.org/10.1016/j.palaeo.2015.05.017.

44) Lymer G., 2014. Interactions entre tectonique crustale, tectonique salifère et sédimentation : la marge occidentale du Bassin Tyrrhénien. Thèse de Doctorat, Université de Lille 1, p. 327.

45) Maillard, A., and Mauffret, A., 2006. Relationship between erosion surfaces and Late Miocene Salinity Crisis deposits in the Valencia Basin (northwestern Mediterranean):

evidence for an early sea-level fall, Terra Nova 18, 321-329, doi: 10.1111/j.1365-3121.2006.00696.x.

46) Maillard, A., and Mauffret, A., 2011. Valencia Basin, in: Lofi, J., Deverchère, J., Gaullier, V., Gillet, H., Gorini, C., Guennoc, P., Loncke, L., Maillard, A., Sage, F. and Thinon, I., 2011. Seismic atlas of the "Messinian Salinity Crisis" markers in the Mediterranean and Black Seas: Commission for the Geological Map of the World (CGMW) / Mémoires de la Société Géologique de France, n.s., 179, 72 pp., 1 CD.

47) Maillard, A., Gorini, C., Mauffret, A., Sage, F, Lofi, J., and Gaullier, V., 2006. Offshore evidence of polyphase erosion in the Valencia Basin (NorthWestern Mediterranean): scenario for the Messinian Salinity Crisis. In: Rouchy, J.M., Suc, J.P., Ferrandini, J., Eds., The Messinian Salinity Crisis re-visited: Sedimentary Geology, 188-189, 69-91, doi: 10.1016/j.sedgeo.2006.02.006.

48) Maillard, A., Driussi, O., Lofi, J., Briais, A., Chanier, F., Hübscher, C., and Gaullier, V., 2014. A complete record of the Messinian markers in the SW Mallorca area (Balearic Promontory, Spain). Marine Geology, 357, 304-302. Doi: 10.1016/j.margeo.2014.10.001.

49) Major, C.O., and Ryan, W.B.F., 1999. Eratosthenes Seamount: Record of late Messinian sea-level changes and facies related to the Messinian Salinity Crisis. Memorie Società Geologica Italiana., 54, 47–59.

50) Malinverno, A., Cafiero, M., Ryan, W. B. F., Cita, M. B., 1981. Distribution of Messinian sediments and erosional surfaces beneath the Tyrrhenian. Sea: geodynamic implications. Oceanologica Acta 1981 - Vol. 4- No 4, 489-495.

51) Malinverno, A., and Ryan, W., 1986. Extension in the Tyrrhenian Sea and shortening in the Apennines as result of arc migration driven by sinking of the lithosphere. Tectonics, 5, 227–245, doi: 10.1029/TC005i002p00227.

52) Manzi, V., Gennari, R., Hilgen, F., Krijgsman, W., Lugli, S., Roveri, M., Sierro, F.J., 2013. Age refinement of the Messinian salinity crisis onset in the Mediterranean. Terra Nova 25, 315–322, doi: 10.1111/ter.12038.

53) Mascle, J., and Réhault, J.P., 1990. A revised seismic stratigraphy of the Tyrrhenian Sea: Implications for the basin évolution. In : Kastens, K. A., Mascle, J., et al.,- Proceedings of the Ocean Drilling Program, Scientific Results, 107, 617-636.

54) Mattei, M., Cipollari, P., Cosentino, D., Argentieri, A., Rossetti, F., Speranza, F., and Di Bella, L., 2002. The Miocene tectono-sedimentary evolution of the southern Tyrrhenian Sea: stratigraphy, structural and palaeomagnetic data from the on-shore Amantea basin (Calabrian Arc, Italy). Basin Research, 14(2), 147-168, doi: 10.1046/j.1365-2117.2002.00173.x.

55) Mauffret, A., Fail, J.P., Montadert, L., Sancho, J., Winnock, E., 1973. Northwestern Mediterranean sedimentary basin from seismic reflection profile. American Association of Petroleum Geologists Bulletin 57, 2245–2262.

56) Mauffret, A., Montadert, L., Lavergne, M., Wilm, C., 1978. Geological and geophysical setting of DSDP Site 372 (Western Mediterranean). In: Montadert, L., Hsü, K.J. (Eds.), Initial Reports of the Deep Sea Drilling Project, vol. 42. U.S. Government Printing Office, Washington DC, pp. 889–896.

57) Mauffret, A., Contrucci, I., Brunet, C., 1999. Structural evolution of the Northern Tyrrhenian Sea from new seismic data. Marine and Petroleum Geology, 16, 381-407, doi: 10.1016/S0264-8172(99)00004-5.

58) MediMap Group, 2008. Morpho-bathymetry of the Mediterranean Sea. CIESM/IFREMER Special Publication, Atlases and Maps, two maps at 1/2000000.

59) Mitchell, N.C., and Lofi, J., 2008. Submarine and subaerial erosion of volcanic landscapes: Comparing the Pacific Ocean seamounts with Valencia Seamount, exposed

during the Messinian Salinity Crisis. Basin Research 20, 489–502, doi: 10.1111/j.1365-2117.2008.00355.x.

60) Mitchum, R., and Vail, P., 1977. Seismic stratigraphy and global change of sea-level, part 7: seismic stratigraphic interpretation procedure. Seismic stratigraphy – Application to hydrocarbon exploration. American Association of Petroleum Geologists Bulletin, 26, 135-143, doi: 10.1306/M26490C9.

61) Montadert, L., Sancho, J., Fial, J.-P. & Debysser, J., 1970. De l'âge tertiaire de la série salifère responsable des structures diapiriques en Méditerranée occidentale (Nord-Est des Baléares). Comptes Rendus de l'Académie des Sciences de Paris, 271, 812-815.

62) Moussat, E., 1983. Evolution de la Mer Tyrrhénienne centrale et orientale et de ses marges septentrionales en relation avec la néotectonique dans l'arc calabrais: Thèse de Doctorat de 3ème Cycle, Université Pierre et Marie Curie, 241 pp.

63) Obone Zue Obame, E., Gaullier, V., Sage, F., Maillard, A., Lofi, J., Vendeville, B., Thinon, I., Réhault, J.-P., and the MAURESC Shipboard Scientific Party, 2011. The sedimentary markers of the Messinian Salinity Crisis and their relation with salt tectonics on the Provençal margin (Western Mediterranean): Results from the "MAURESC" cruise. Special Issue « Miocene-Pliocene geodynamics and paleogeography in the Mediterranean region: eustasy-tectonics interference »: Bulletin de la Société géologique de France, 182 (2), 181-196, doi: 10.2113/gssgfbull.182.2.181.

64) Ochoa, D., Sierro, F. J., Lofi, J., Maillard, A., Flores, J.A., and Suarez, M., 2015. Synchronous onset of the Messinian evaporite precipitation: First Mediterranean offshore evidence. Earth and Planetary Science Letters, 427, 112-124, doi.org/10.1016/j.epsl.2015.06.059.

65) Panieri, G., Lugli, S., Manzi, V., Roveri, M., Schreiber, C.B., and Palinska, K.A., 2010, Ribosomal RNA gene fragments from fossilized cyanobacteria identified in primary

gypsum from the late Miocene, Italy: Geobiology, v. 8, p. 101–111, doi:10.1111/j.1472-4669.2009.00230.x.

66) Popescu, S.-M., Dalibard, M., Suc, J.-P., Barhoun, N., Melinte-Dobrinescu, M.-C., Bassetti, M.,-A., Deaconu, F., Head, M.J., Gorini, C., Do Couto, D., Rubino, J.-L., Auxietre, J.-L., Floodpage, J., 2015. Lago Mare episodes around the Messinian-Zanclean boundary in the deep southwestern Mediterranean. Marine and Petroleum Geology, Volume 66, Part 1, September 2015, Pages 55-70, https://doi.org/10.1016/j.marpetgeo.2015.04.002.

67) Prada, M., Ranero, C.R., Sallarès, V., Zitellini, N., Grevemeye, I., 2016. Mantle exhumation and sequence of magmatic events in the Magnaghi–Vavilov Basin (Central Tyrrhenian, Italy): New constraints from geological and geophysical observations. Tectonophysics, 689, 2016, Pages 133-142, https://doi.org/10.1016/j.tecto.2016.01.041

68) Réhault, J.P., Boillot, G., Mauffret, A., 1984. The western Mediterranean basin, geological evolution. Marine Geology, 55, 447-477, doi: 10.1016/0025-3227(84)90081-1.

69) Réhault, J.P., Mascle, J., Fabbri, A., Moussat, E., Thommeret, M., 1987. The Tyrrhenian Sea before LEG 107. In : Kastens, K.A., Mascle, J., Auroux, C., et al., 1987. Proceedings of the Ocean Drilling Program, Part A., Initial Reports, Sites 650 – 656. Ocean Drilling Program, College Station, TX, 107, 772 pp.

70) Rossi M., Minervini M., Ghielmi M., Rogledi S., 2015. Messinian and Pliocene erosional surfaces in the Po Plain-Adriatic Basin: Insights from allostratigraphy and sequence stratigraphy in assessing play concepts related to accommodation and gateway turnarounds in tectonically active margins. Marine and Petroleum Geology, Volume 66, Part 1, September 2015, Pages 192-216, https://doi.org/10.1016/j.marpetgeo.2014.12.012

71) Rouchy, J.-M., and Caruso, A., 2006. The Messinian salinity crisis in the Mediterranean basin: a reassessment of the data and an integrated scenario. Sedimentary Geology, 188-189, 35-67, 10.1016/j.sedgeo.2006.02.005.

72) Roveri, M., Lugli, S., Manzi, V., and Schreiber, B.C., 2008. The Messinian Sicilian stratigraphy revisited: new insights for the Messinian Salinity Crisis. Terra Nova, 20, 483-488, doi : 10.1111/j.1365-3121.2008.00842.x.

73) Roveri, M., Lugli, S., Manzi, V., Gennari, R., Schreiber, B.C., 2014a. High resolution strontium isotope stratigraphy of the Messinian deep Mediterranean basins: Implications for marginal to central basins correlation. Marine Geology, doi: 10.1016/j.margeo.2014.01.002

74) Roveri, M., Flecker, R., Krijgsman, W., Lofi, J., Lugli, S., Manzi, V., Sierro, F.J., Bertini, A., Camerlenghi, A., De Lange, G., Govers, R., Hilgen, F.J., Hübscher, C., Meijer, P.Th., Stoica, M., 2014b. The Messinian Salinity Crisis: Past and duture of a great challenge for marine sciences. Marine Geology, http://dx.doi.org/10.1016/j.margeo.2014.02.002

75) Roveri, M., Manzi, V., Bergamasco, A., Falcieri, F., Gennari, R. & Lugli, S. 2014c. Dense shelf water cascading and Messinian canyons: a new scenario for the Mediterranean salinity crisis. American Journal of Science, 314, 751–784, doi: 10.2475/05.2014.03.

76) Roveri, M., Gennari, R., Lugli, S., Manzi, V., Minelli, N., Reghizzi, M., Riva, A., Rossi, M. E., Schreiber, B.C., 2016. The Messinian Salinity Crisis: open problems and possible implications for Mediterranean petroleum systems. Petroleum Science, volume 22, 4, 283-290, doi: 10.1144/petgeo2015-089.

77) Ryan, W.B.F., 1973. Geodynamic implication of the Messinian crisis of salinity. In: C.W. Drooger, Ed., Messinian events in the Mediterranean. North-Holland Publishing Company, Amsterdam, 26-28.

78) Ryan, W.B.F., 2011. Geodynamics responses to a two-step model of the Messinian Salinity Crisis. Bulletin de la Société Géologique de France, 182 (2), 73–78, 10.2113/gssgfbull.182.2.73.

79) Ryan, W.B.F., and Stanley, D.J., 1971. The tectonics and geology of the Mediterranean Sea. In: Maxell, A. (Ed.), The Sea, vol. 4. Wiley, New York. 387 pp.

80) Ryan, W.B.F., Hsü, K.J., Cita, M.B., and the shipboard scientific party, 1973. Tyrrhenian rise - site 132. DSDP Volume XIII, 61, 403-464, doi: 10.2973/dsdp.proc.13.114.1973

81) Ryan, W.B.F., Cita, M.B., 1978. The nature and distribution of Messinian erosional surface: indication of a several-kilometer-deep Mediterranean in the Miocene. Marine Geology 27, 193–230, 10.1016/0025-3227(78)90032-4.

82) Sage, F., Von Gronefeld, G., Deverchere, J., Gaullier, V., Maillard, A. and Gorini, C., 2005. Seismic evidence for Messinian detrital deposits at the Western Sardinia margin, northwestern Mediterranean. Marine and Petroleum Geology, 22, 757-773. 10.1016/j.marpetgeo.2005.03.007.

83) Sage, F., and Déverchère, J., 2011. Northern Ligurian, in: Lofi, J., Deverchère, J., Gaullier, V., Gillet, H., Gorini, C., Guennoc, P., Loncke, L., Maillard, A., Sage, F. and Thinon, I., 2011, Seismic atlas of the "Messinian Salinity Crisis" markers in the Mediterranean and Black Seas: Commission for the Geological Map of the World (CGMW) / Mémoires de la Société Géologique de France, n.s., 179, 72 pp., 1 CD.

84) Sage, F., Déverchère, J., Von Gronefeld, G., Gaullier, V., Gorini, C., Maillard, A. and Cornée, J.-J., 2011. Western Tyrrhenian, in: Lofi, J., Deverchère, J., Gaullier, V., Gillet, H., Gorini, C., Guennoc, P., Loncke, L., Maillard, A., Sage, F. and Thinon, I., 2011,

Seismic atlas of the “Messinian Salinity Crisis” markers in the Mediterranean and Black Seas: Commission for the Geological Map of the World (CGMW) / Mémoires de la Société Géologique de France, n.s., 179, 72 pp., 1 CD.

85) Sartori, R., 1990. The main results of the ODP Leg 107 in the frame of Neogene to recent geology of perytyrrhenian areas. In: Kastens K., Mascle J. et al. Eds., Proceedings of the Ocean Drilling Program, Scientific Results. 107, 715-730. College Station, TX, doi:10.2973/odp.proc.sr.107.183.1990.

86) Sartori, R., 2003. The Tyrrhenian back-arc basin and subduction of the Ionian lithosphere. Episodes, Vol. 26, N°3, 217-221.

87) Sartori, R., Carrara, G., Torelli, L., Zitellini, N., 2001. Neogene evolution of the southwestern Tyrrhenian Sea (Sardinia Basin and Western bathyal plain): Marine Geology, 175, 47–66, doi: 10.1016/S0025- 3227(01)00116-5.

88) Sartori, R., Torelli, L., Zitellini, N., Carrara, G., Magaldi, M., Mussoni, P., 2004. Crustal features along a W-E Tyrrhenian transect from Sardinia to Campania margins (Central Mediterranean). Tectonophysics, 383, 171-192, 10.1016/j.tecto.2004.02.008.

89) Stampfli, G.M. and Höcker, C.F.W., 1989. Messinian palaeorelief from 3-D seismic survey in the Tarraco concession area (Spanish Mediterranean sea): Geologie en Mijnbouw, 68, 2, 201-210.

90) Thinon, I., Guennoc, P., Serrano, O., Maillard, A., Lasseur, E., Réhault, J.P., 2016. Seismic markers of the Messinian Salinity Crisis in an intermediate-depth basin: data for understanding the Neogene evolution of the Corsica Basin (Northern Tyrrhenian Sea). Marine and Petroleum Geology, Volume 77, November 2016, Pages 1274–1296. Doi : 10.1016/j.marpetgeo.2016.02.017.

91) Thomas, B., Lecca, L., Gennesseaux, M., 1988. Structuration et morphogenèse de la marge occidentale de la Sardaigne au Cénozoïque. Compte Rendu de l'Académie des Sciences de Paris, 306 (Série. II), 903–910.

92) Thommeret, M., 1990. Tectonique comparée des marges continentales sarde (Mer Tyrrhénienne, Italie) et galicienne (Nord-Ouest de l'Ibérie). Thèse de Doctorat de l'Université Pierre et Marie Curie, 325 pp.

93) Urgeles, R., Camerlenghi, A., Garcia-Castellanos, D., De Mol, B., Garcés, M., Vergés, J., Haslama, I., Hardman, M., 2011. New constraints on the Messinian sea level drawdown from 3D seismic data of the Ebro Margin, western Mediterranean. Basin Research 23, 123–145, doi: 10.1111/j.1365-2117.2010.00477.x.

94) Vai, G.B., and Martini, I.P., 2001. Anatomy of an orogen: Northern Apennines and Adjacent Mediterranean Basins. Kluwer Academic Publication, Dordrecht, 632 pp.

95) Vendeville, B.C., and Cobbold, P., 1987. Glissements gravitaires synsédimentaires et failles normales listriques : modèles expérimentaux. Compte Rendu de l'Academie des Sciences de Paris, t. 305, Série II, p. 1313-1319.

FIGURE CAPTIONS:

Figure 1. Bathymetric map of the study area (modified from the DTM published by the CIESM/Ifremer Medimap Group et al., 2008) and tectonic structures in the Eastern Sardinian Margin from the METYSS seismic surveys (modified from Thommeret, 1990; Vai and Martini, 2001; Sartori et al., 2001; Carrara, 2002; Lymer, 2014). Location of the Orosei Canyon Line (OCL), Circeo/41° North Fault from Sartori et al. (2001) and Mauffret et al. (1999)**.** Isobath equidistance: 100 m. Red lines correspond to the location of the "METYSS 1" and "METYSS 3" seismic lines. Thick red lines indicate the position of the « METYSS » seismic profiles shown in this work. White dots: ODP and DSDP drilling sites, from Kastens et al. (1988) and Ryan et al. (1973) and core BS77-19 from Sartori et al. (2001).

Figure 2. Seismo-stratigraphic column of the study area from the ODP sites 653, 654 and DSDP site 132 (see location on Figure 1). A: MYS12 seismic line correlated with stratigraphic column of the Leg 107 ODP drill 654 (Modified from Mascle and Réhault, 1990, and Gaullier et al., 2014). Fan-shaped, blue reflectors correspond to the syn-rift deposits. The red arrows underline the onlap of the UU on the BES. Thicknesses are in stwtt. B: MS-1 seismic line correlated with stratigraphy of the Leg 107 ODP drill 653 and DSDP 132 (Modified from Ryan et al., 1973).

Figure 3. Schematic cross section of the Western Mediterranean Basin, illustrating the geometric organization of the MSC seismic markers at the end of the MSC. The impact of salt tectonics is not taken in account. The figure also illustrates the different status of the MSC basins during the MSC. (Modified from Lofi et al., 2011a, b, and Ochoa et al., 2015). MSC units and surfaces from Lofi et al., (2011a and 2011b): MES: Margin Erosion Surface; TS/TES: Top (Erosion) Surface; BS/BES: Bottom (Erosion) Surface; BU: Bedded Unit; CU: Complex Unit; LU: Lower Unit; MU: Mobile Unit; UU: Upper Unit. MSC units from Roveri et al., 2016: PLG: Primary Lower Gypsum.

Figure 4. Uninterpreted (A) and interpreted (B) seismic profile MYS51b, located on the western side of the East-Sardinia Basin, illustrating the Margin Erosion Surface (MES) on the continental slope. Also note the post-rift (in pink) and syn-rift (in blue) pre-MSC deposits. Thicknesses are in stwtt. See text for details and Figure 1 for location.

Figure 5. Uninterpreted (A) and interpreted (B) seismic profile MYS40 illustrating the transition between the East-Sardinia Basin and the Cornaglia Terrace, separated by the Quirra Seamounts. The MSC units (UU and MU) accumulated in both basins. The MES is present on the seamount. Note the presence of crustal normal faults and syn-rift pre-MSC deposits (in blue) below the MES. The faults do not affect the MSC markers. See text for details and Figure 1 for location.

Figure 6. MSC line ST08 (A) from Sartori et al. (2001), compared with uninterpreted (B) and interpreted (C) seismic profile MYS47 accross the East-Sardinia Basin and the western side of the Cornaglia Terrace. (D) Close up on the Margin Erosion Surface (MES). (E) Close up showing the unusual seismic facies of the UU, labelled "chaotic UU" there. See text for details and Figure 1 for location.

Figure 7. Uninterpreted (A) and interpreted (B) seismic profile MYS14, illustrating the onlap of the MSC deposits on the Baronie Ridge in the northern East-Sardinia Basin. The series from the pre-MSC to the Early Pliocene are gently folded, showing post-MSC tectonic activity. See text for details and Figure 1 for location (modified from Gaullier et al., 2014).

Figure 8. Uninterpreted (A) and interpreted (B) seismic profile MYS54, located east of the Baronie Ridge in the northern Cornaglia Terrace. The Margin Erosion Surface (MES) is on the Onifai Ridge and the MSC deposits (UU, MU) in the basin. To the north, the UU onlaps on the Onifai Ridge. See text for details and Figure 1 for location.

Figure 9. Uninterpreted (A) and interpreted (B) seismic profile MYS24, illustrating the northern East-Sardinia Basin. The MES is observed on the upper-slope and on the isolated Caprera Ridge. The offset of the MSC seismic markers highlight post-MSC tectonic activity. See text for details and Figure 1 for location.

Figure 10. Present-day distribution map of the Margin Erosion Surface (MES) and the MSC units (Mobile Unit: MU; Upper Unit: UU). The depth contours of the top of MES and top of UU, *i.e.* the base of Plio-Quaternary formation, are indicated from the METYSS dataset and previous works by Curzi et al. (1980) [MU: "lower sequence"; UU: "upper sequence"], Moussat (1983) [MU: facies n° 6 and 7; UU: facies n°2] and Thinon et al., 2016 [MES, BU and syn-MSC paleovalleys of the East-Corsica basin]. The grey lines show the location of the METYSS dataset.

Figure 11. Uninterpreted (A) and interpreted (B) seismic profile MYS09a, illustrating the UU and MU on the Cornaglia Terrace. The presence of the MES on the structural highs is indicated as probable because of the absence of clear connexion with MSC deposits. Salt tectonics affects the MU and the UU. See text for details and Figure 1 for location (modified from Gaullier et al., 2014).

Figure 12. Thickness map of the Upper Unit (UU). The UU is thin in the East-Sardinia Basin, compared to the Cornaglia Terrace. We used a mean internal velocity of 3500 m/s in the UU for time-to-depth conversion of the thickness scale (Réhault et al., 1984).

Figure 13. Uninterpreted (A) and interpreted (B) seismic profile MYS11 illustrating the seismic facies of the "chaotic UU" in the Orosei Canyon area. C and D. Closes up on the "chaotic UU" seismic facies. The faults in the UU and the PQ above the MU are related to salt tectonics, *i.e.* gravity gliding. See text for details and Figure 1 for location.

Figure 14. Uninterpreted (A) and interpreted (B) seismic profile MYS37 illustrating the impact of salt tectonics in the southern Cornaglia Terrace. The UU onlaps onto the Quirra seamounts. See text for details and Figure 1 for location.

Figure 15. Distribution and depth of the top of the Mobile Unit (MU, modified from Curzi et al., 1980; Moussat, 1983; Gaullier et al., 2014). The top of the MU is clearly deeper in the Cornaglia Terrace than in the East-Sardinia basin.

Figure 16. Part of the seismic profile MYS53, illustrating the presence of the Complex Unit (CU) interfingered with the UU and MU at the southeast foot of the Baronie Ridge. See Figure 1 for location.

Figure 17. Shematic cross-sections based on the interpretation of the METYSS data summarizing the present-day setup of the MSC seismic markers across the Eastern Sardinian margin. Section A is located in the Orosei Canyon area and section B in the southern East-Sardinia Basin and Cornaglia Terrace. Both sections show that the MSC markers are post-rift

across the margin and that the onlap of the MSC units UU and MU on the structural highs deepens eastward. See text for details and Figure 1 for location.

Figure 18. Shematic cross-sections of the Algero-Provencal Basin. Section A is across the Western Sardinian margin (Sage et al., 2011). Section B is across the Provencal margin (Obone Zue Obame et al., 2011). The comparison between the Western Tyrrhenian Basin and the Algero Provencal basins highlight strong similitudes in term of MSC records in both basins.

Research highlights

- Characterization and mapping of the seismic markers of the Messinian Salinity Crisis along the Eastern Sardinian margin.
- Relations between tectonics and sedimentation in the Western Tyrrhenian Basin
- Refining the timing of the rifting in the Western Tyrrhenian Basin.
- Morphology of the Western Tyrrhenian Basin during the Messinian Salinity Crisis.
- Evolution of the Eastern Sardinian margin from rifting to present-day.

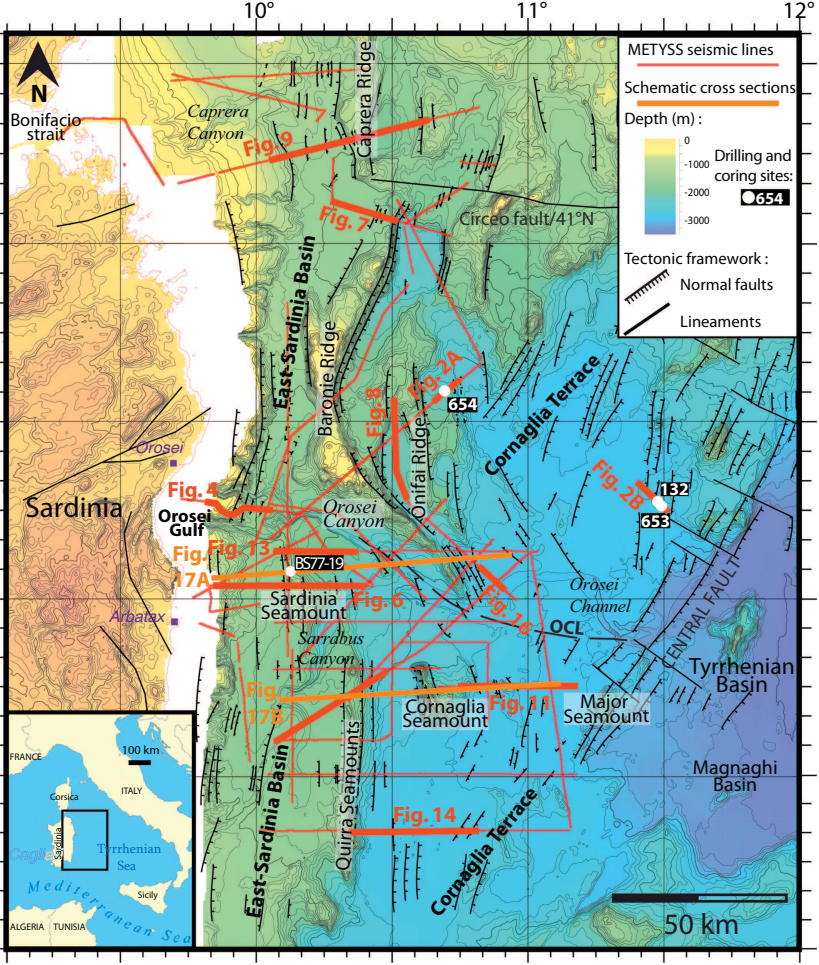
10°
11°
12°
41°
40°
39°
N
Bonifacio strait
Caprera Canyon
Caprera Ridge
Fig. 9
Fig. 7
Circeo fault/41°N
East-Sardinia Basin
Baronie Ridge
Fig. 8
Fig. 2A
654
Onifai Ridge
Cornaglia Terrace
Fig. 2B
132
653
Orosei
Sardinia
Orosei Gulf
Fig. 4
Orosei Canyon
Fig. 13
Fig. 17A
BS7-19
Sardinia Seamount
Fig. 6
Fig. 16
Orosei Channel
OCL
CENTRAL FAULT
Arbatax
Sarrabus Canyon
Fig. 17B
Cornaglia Seamount
Fig. 11
Major Seamount
Tyrrhenian Basin
Magnaghi Basin
Quirra Seamounts
Fig. 14
East-Sardinia Basin
Cornaglia Terrace
50 km
METYSS seismic lines
Schematic cross sections
Depth (m) :
0
-1000
-2000
-3000
Drilling and coring sites:
654
Tectonic framework :
Normal faults
Lineaments
FRANCE
100 km
ITALY
Corsica
Sardinia
Tyrrhenian Sea
Sicily
Mediterranean Sea
ALGERIA
TUNISIA

Figure 1

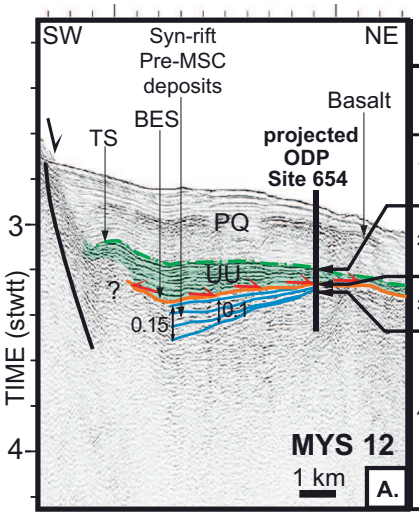

Seismic units (This study)	Lithostratigraphic units (Kastens et al., 1988; Kastens, 1992)	Lithology	Age
1 (post-rift)	Unit I	Nannofossil and foraminifer ooze with a layer of basalt	Pliocene/ Pleistocene
2 (post rift ? syn-rift ?)	Unit II Unit III	Interbedded gypsum cycles Interbedded claystone/siltstone	Messinian (MSC related deposits)
3 (syn-rift)	Unit IV Unit V	Marine nannofossil shalk Nearshore sands	Early-Messinian / Tortonian
4 (pre-rift)	Unit VI	Continental Alluvial fan	Unknown

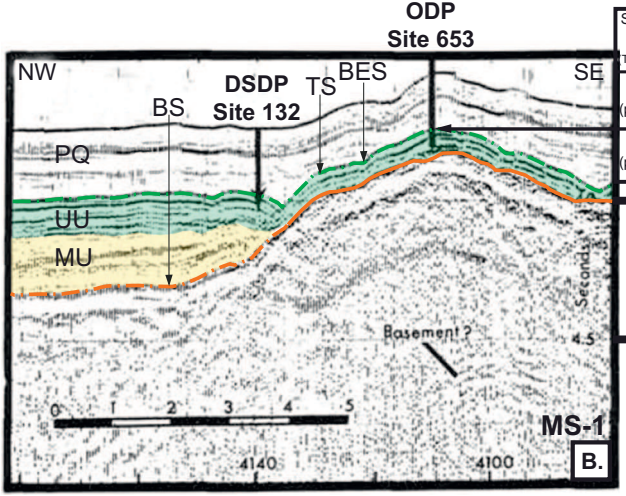

Seismic units This study)	Lithostratigraphic units (Kastens et al., 1988; Kastens, 1992)	Lithology	Age
1 (post-rift)	Unit I	Nannofossil and foraminifer ooze	Pliocene/ Pleistocene
2 (post-rift)	Unit II	Interbedded gypsum cycles	Messi-nian (MSC)

Figure 2

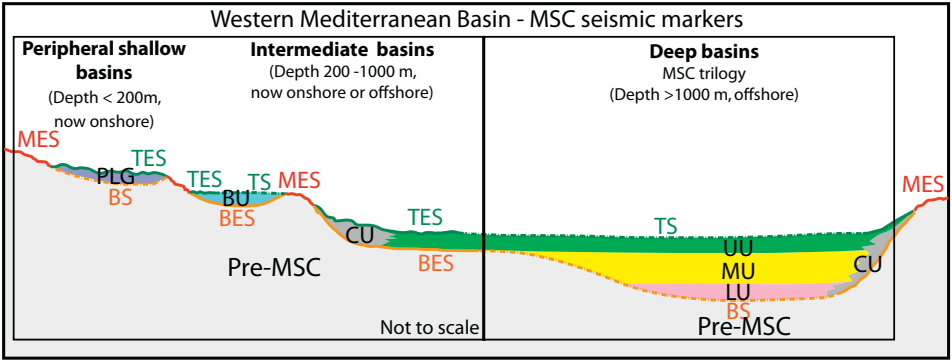
Western Mediterranean Basin - MSC seismic markers
Peripheral shallow basins
(Depth < 200m, now onshore)
Intermediate basins
(Depth 200 -1000 m, now onshore or offshore)
Deep basins
MSC trilogy
(Depth >1000 m, offshore)
MES
TES
PLG
BS
TES
TS
MES
BU
BES
TES
CU
Pre-MSC
BES
Not to scale
TS
UU
MU
LU
BS
Pre-MSC
CU
MES

Figure 3

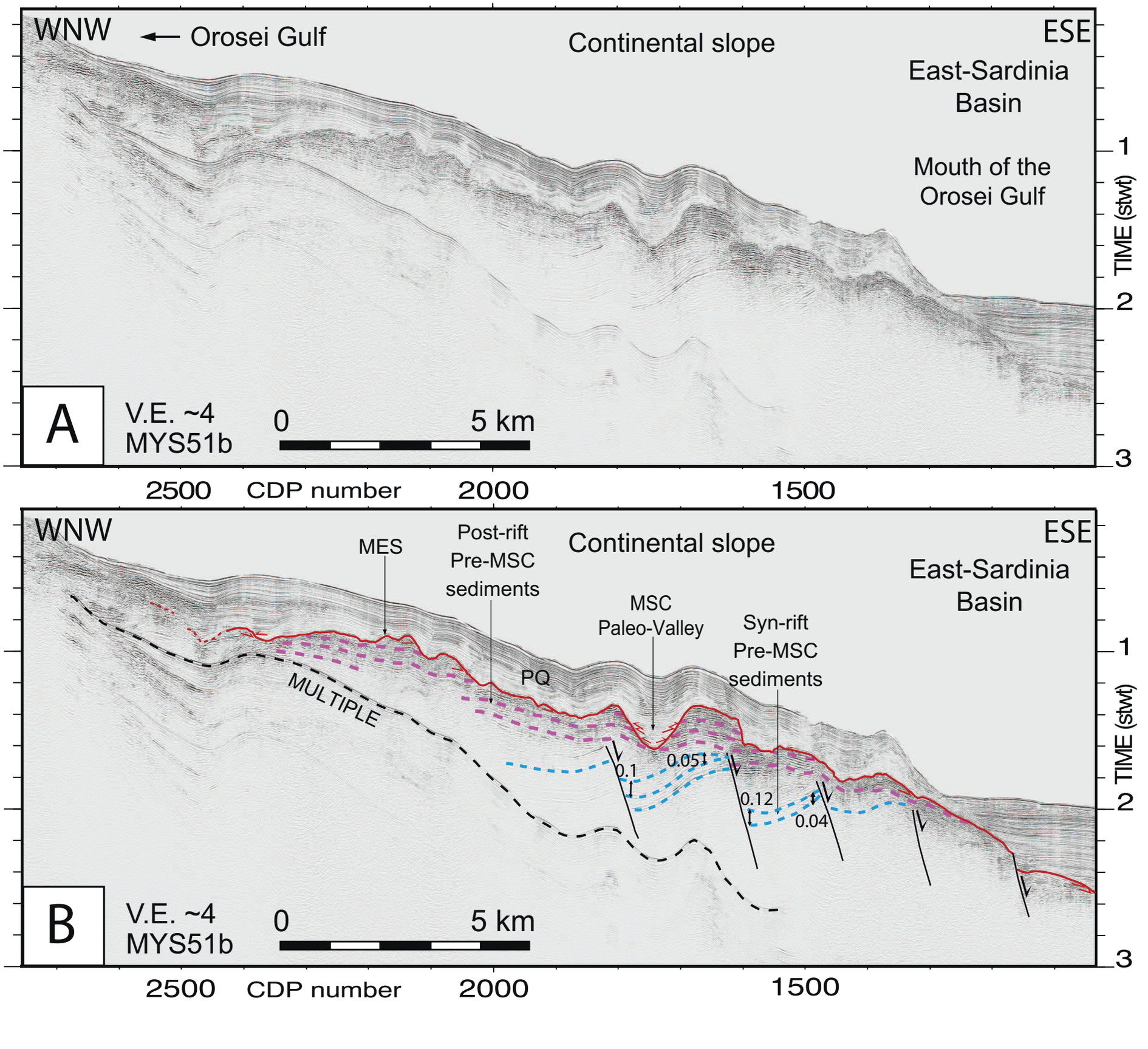
WNW
Orosei Gulf
Continental slope
ESE
East-Sardinia Basin
Mouth of the Orosei Gulf
TIME (stwt)
1
2
3
A
V.E. ~4
MYS51b
0
5 km
2500
CDP number
2000
1500
WNW
MES
Post-rift Pre-MSC sediments
Continental slope
ESE
East-Sardinia Basin
MSC Paleo-Valley
Syn-rift Pre-MSC sediments
PQ
MULTIPLE
0.1
0.05
0.12
0.04
TIME (stwt)
1
2
3
B
V.E. ~4
MYS51b
0
5 km
2500
CDP number
2000
1500

Figure 4

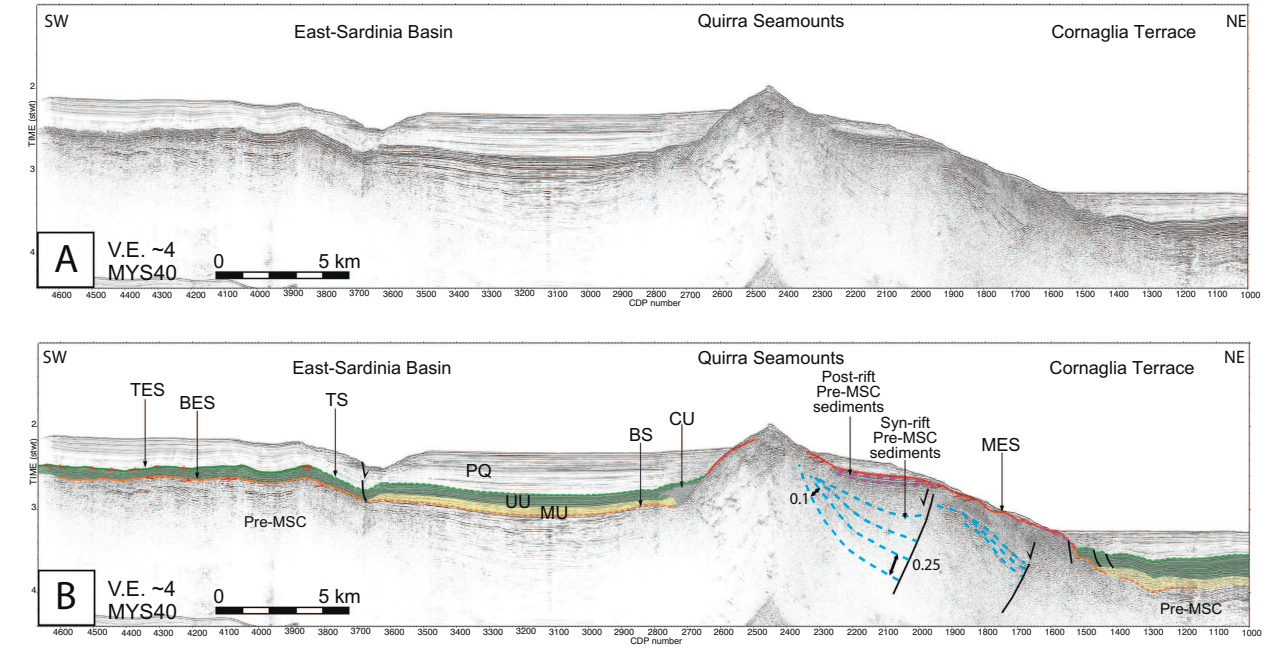
SW
East-Sardinia Basin
Quirra Seamounts
Cornaglia Terrace
NE
TIME (stwt)
A
V.E. ~4
MYS40
0
5 km
CDP number
SW
East-Sardinia Basin
Quirra Seamounts
Cornaglia Terrace
NE
TES
BES
TS
BS
CU
Post-rift
Pre-MSC
sediments
Syn-rift
Pre-MSC
sediments
MES
PQ
UU
MU
Pre-MSC
0.1
0.25
Pre-MSC
B
V.E. ~4
MYS40
0
5 km
CDP number

Figure 5

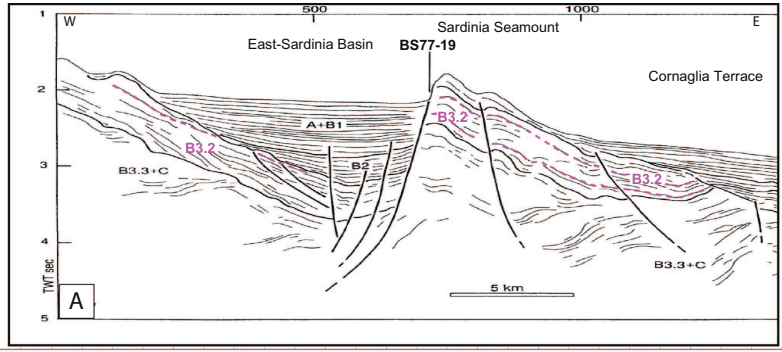
W
E
500
1000
Sardinia Seamount
East-Sardinia Basin
BS77-19
Cornaglia Terrace
A+B1
B3.2
B3.3+C
B2
B3.2
B3.2
B3.3+C
5 km
TWT sec
A

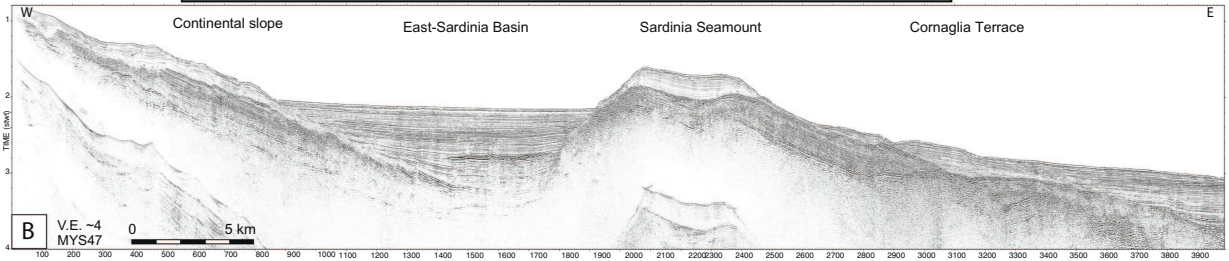
W
E
Continental slope
East-Sardinia Basin
Sardinia Seamount
Cornaglia Terrace
TIME (dsvl)
B
V.E. ~4
MYS47
0
5 km
CDP number

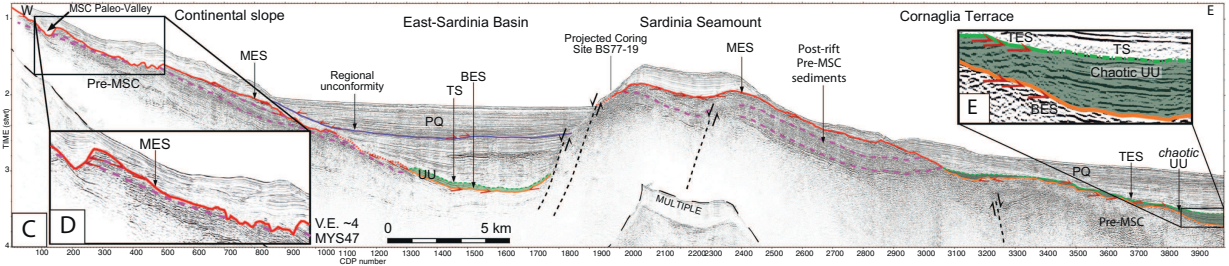
W
E
MSC Paleo-Valley
Continental slope
East-Sardinia Basin
Sardinia Seamount
Cornaglia Terrace
Pre-MSC
MES
Regional unconformity
BES
TS
PQ
UU
Projected Coring Site BS77-19
MES
Post-rift Pre-MSC sediments
MULTIPLE
TES
TS
Chaotic UU
BES
E
TES
chaotic UU
PQ
Pre-MSC
C
D
MES
V.E. ~4
MYS47
0
5 km
TIME (dsvl)
CDP number

Figure 6

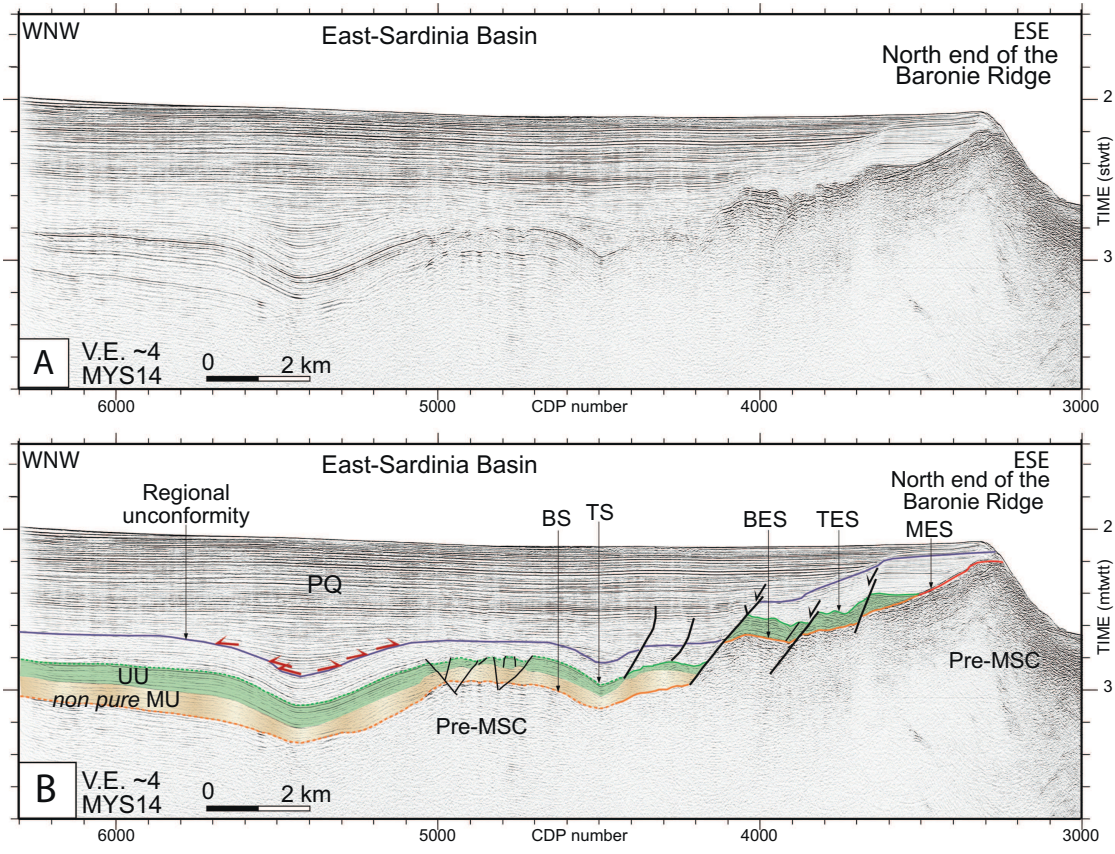
WNW
East-Sardinia Basin
ESE
North end of the
Baronie Ridge
TIME (stwt)
2
3
A
V.E. ~4
MYS14
0
2 km
6000
5000
CDP number
4000
3000
WNW
East-Sardinia Basin
ESE
North end of the
Baronie Ridge
Regional
unconformity
BS
TS
BES
TES
MES
PQ
UU
non pure MU
Pre-MSC
Pre-MSC
TIME (mtwt)
2
3
B
V.E. ~4
MYS14
0
2 km
6000
5000
CDP number
4000
3000

Figure 7

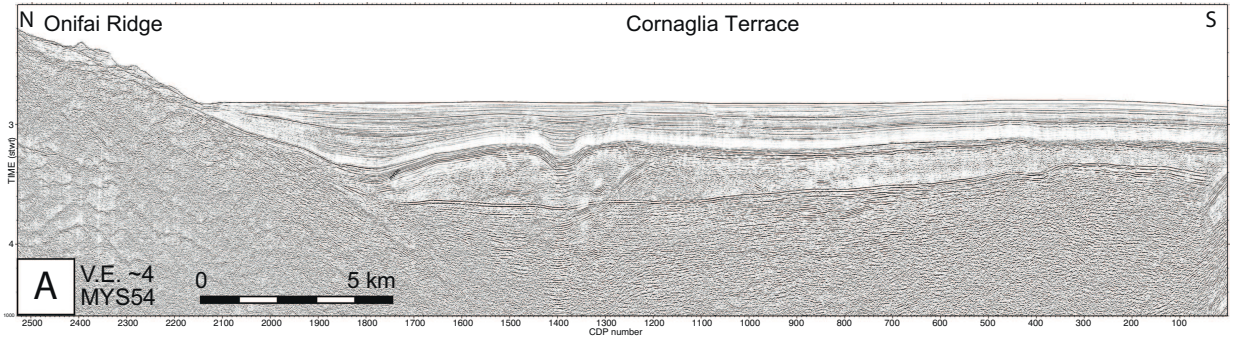
N
Onifai Ridge
Cornaglia Terrace
S
TIME (sec)
3
4
A
V.E. ~4
MYS54
0
5 km
2500 2400 2300 2200 2100 2000 1900 1800 1700 1600 1500 1400 1300 1200 1100 1000 900 800 700 600 500 400 300 200 100
CDP number

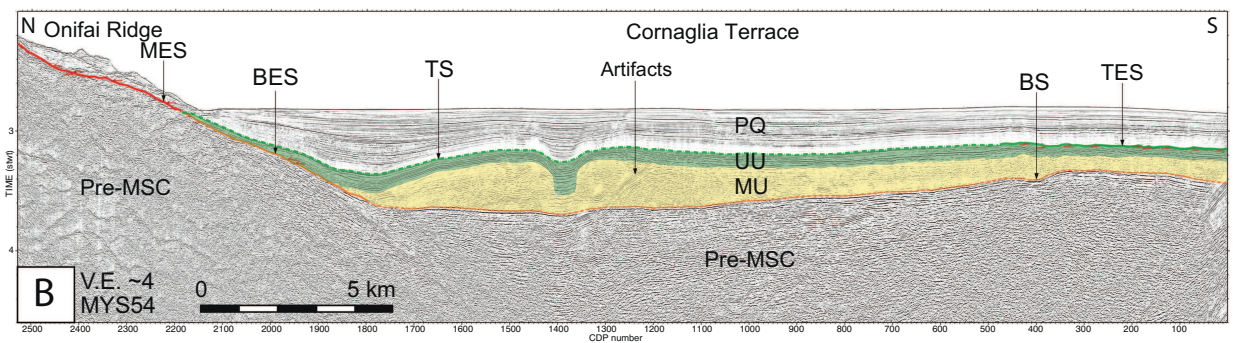
N
Onifai Ridge
Cornaglia Terrace
S
MES
BES
TS
Artifacts
BS
TES
PQ
UU
MU
Pre-MSC
Pre-MSC
TIME (sec)
3
4
B
V.E. ~4
MYS54
0
5 km
2500 2400 2300 2200 2100 2000 1900 1800 1700 1600 1500 1400 1300 1200 1100 1000 900 800 700 600 500 400 300 200 100
CDP number

Figure 8

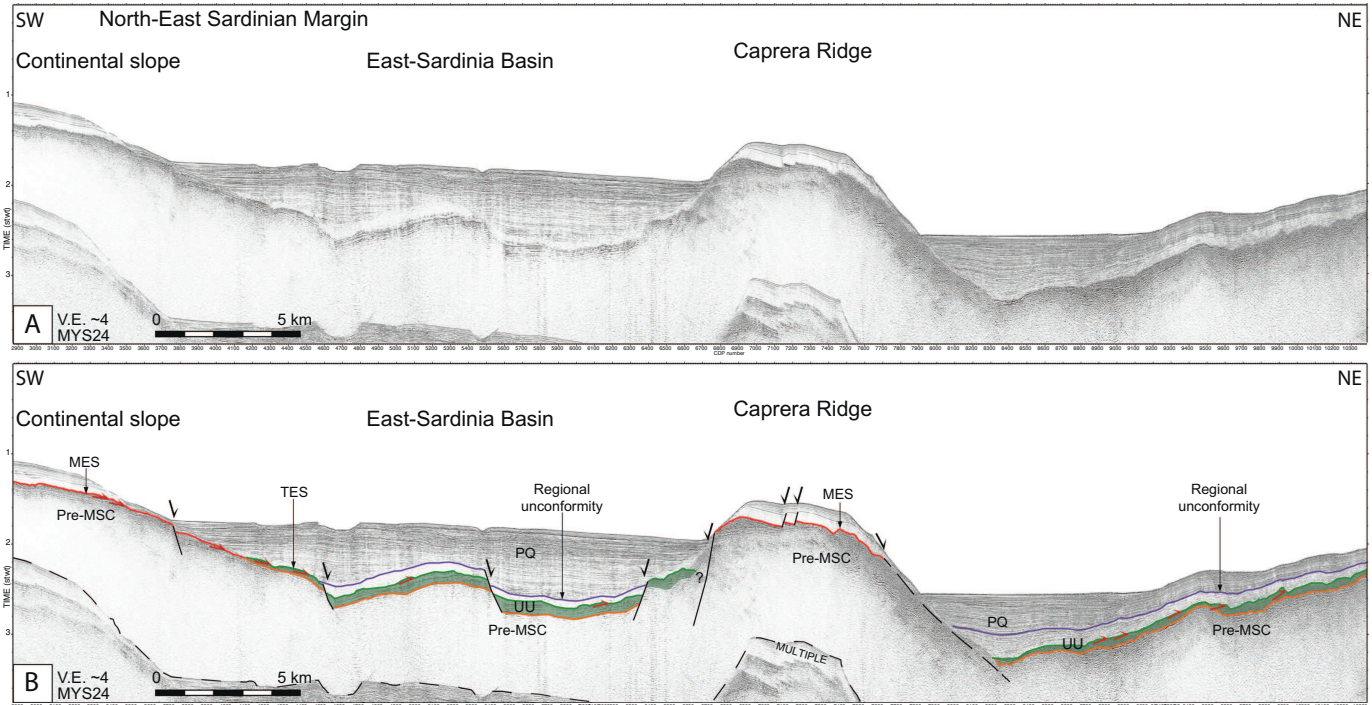
SW
North-East Sardinian Margin
NE
Continental slope
East-Sardinia Basin
Caprera Ridge
TIME (s/w)
A
V.E. ~4
MYS24
0
5 km
CDP number
SW
NE
Continental slope
East-Sardinia Basin
Caprera Ridge
MES
Pre-MSC
TES
Regional unconformity
PQ
UU
Pre-MSC
?
MES
Pre-MSC
Regional unconformity
PQ
UU
Pre-MSC
MULTIPLE
B
V.E. ~4
MYS24
0
5 km
CDP number

Figure 9

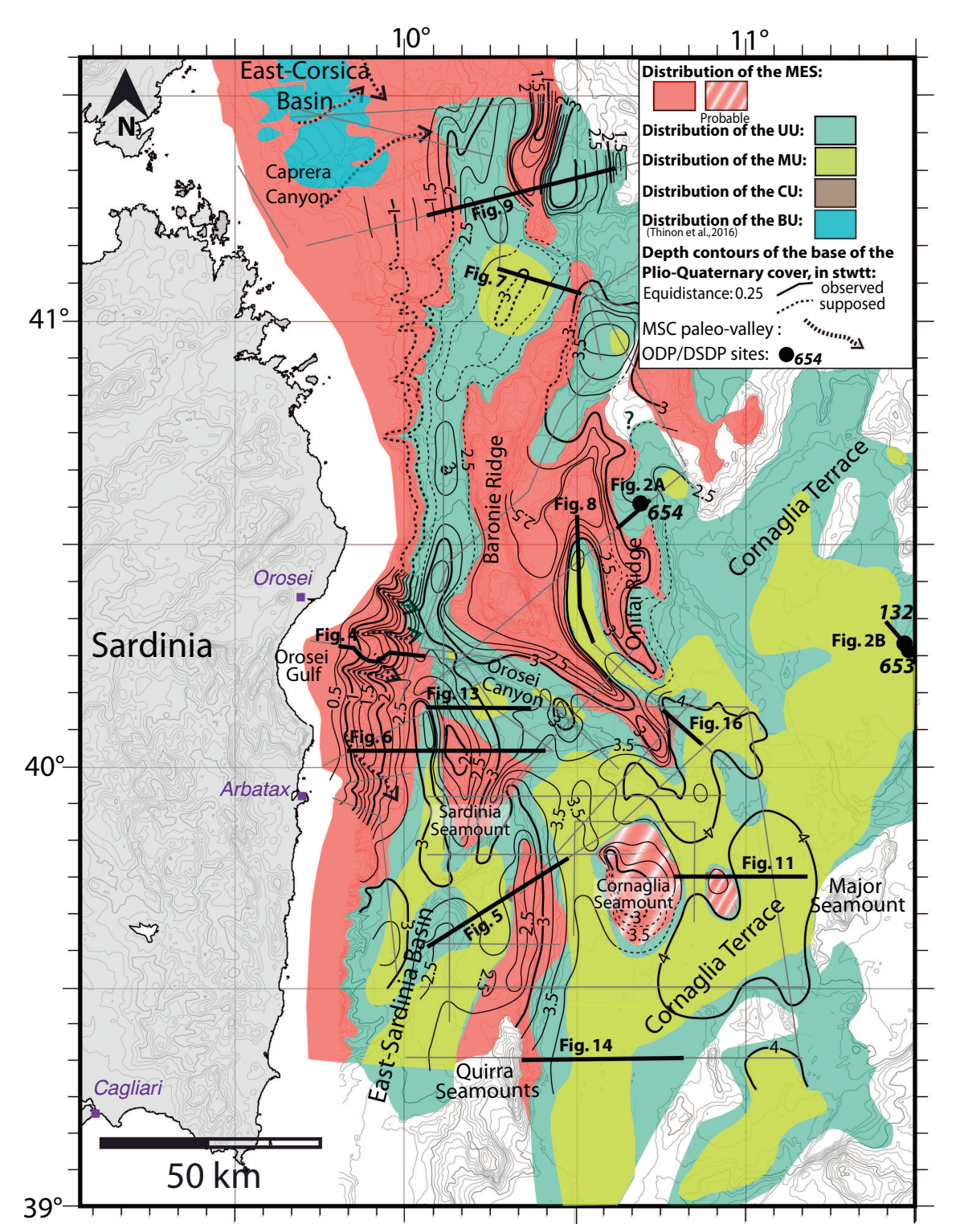
10°
11°
41°
40°
39°
East-Corsica Basin
Caprera Canyon
N
Sardinia
Orosei
Arbatax
Cagliari
50 km
Orosei Gulf
Baronie Ridge
Onifai Ridge
Cornaglia Terrace
Orosei Canyon
Sardinia Seamount
Cornaglia Seamount
Major Seamount
East-Sardinia Basin
Quirra Seamounts
Fig. 1
Fig. 2A
Fig. 2B
Fig. 4
Fig. 5
Fig. 6
Fig. 7
Fig. 8
Fig. 9
Fig. 11
Fig. 13
Fig. 14
Fig. 16
654
653
132
Distribution of the MES:
Probable
Distribution of the UU:
Distribution of the MU:
Distribution of the CU:
Distribution of the BU:
(Thinon et al.,2016)
Depth contours of the base of the Plio-Quaternary cover, in stwtt:
Equidistance: 0.25
observed
supposed
MSC paleo-valley :
ODP/DSDP sites:

Figure 10

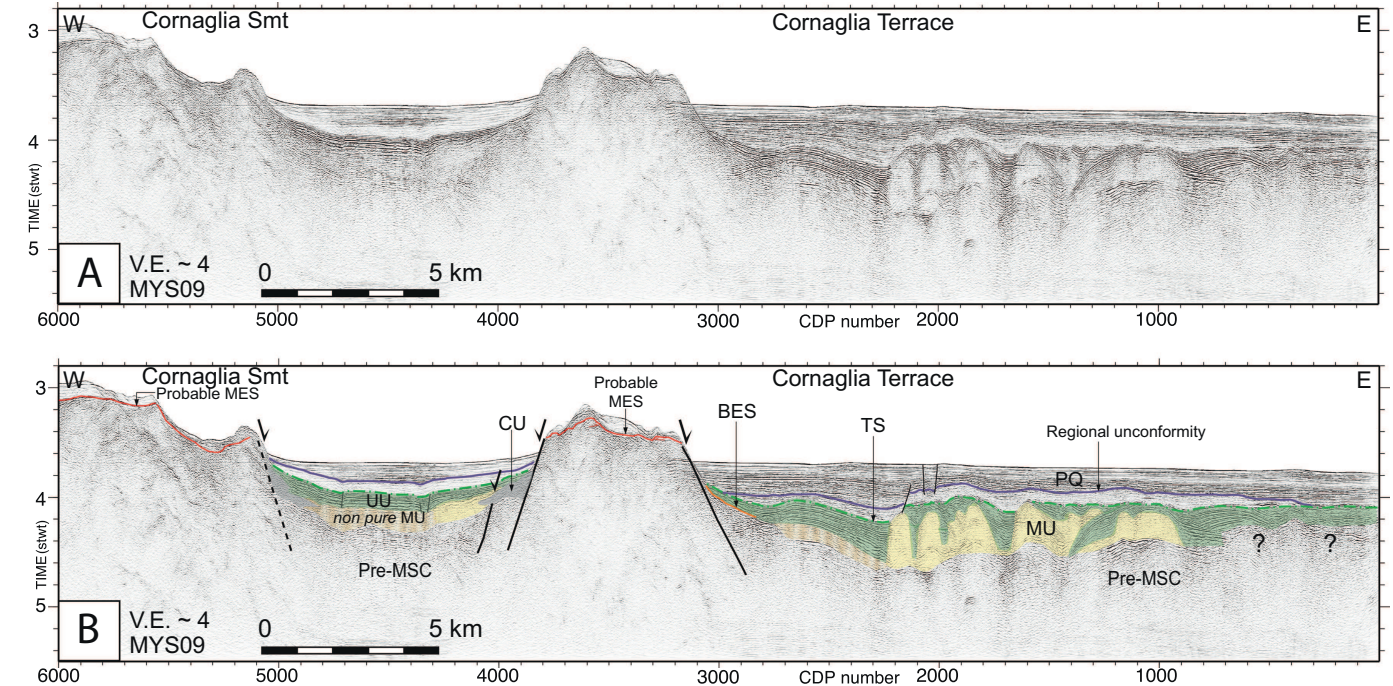
W
Cornaglia Smt
Cornaglia Terrace
E
TIME (stwt)
3
4
5
A
V.E. ~ 4
MYS09
0
5 km
6000
5000
4000
3000
CDP number
2000
1000
W
Cornaglia Smt
Probable MES
Probable MES
CU
BES
TS
Regional unconformity
Cornaglia Terrace
E
PQ
UU
non pure MU
MU
Pre-MSC
Pre-MSC
?
?
B
V.E. ~ 4
MYS09
0
5 km
CDP number

Figure 11

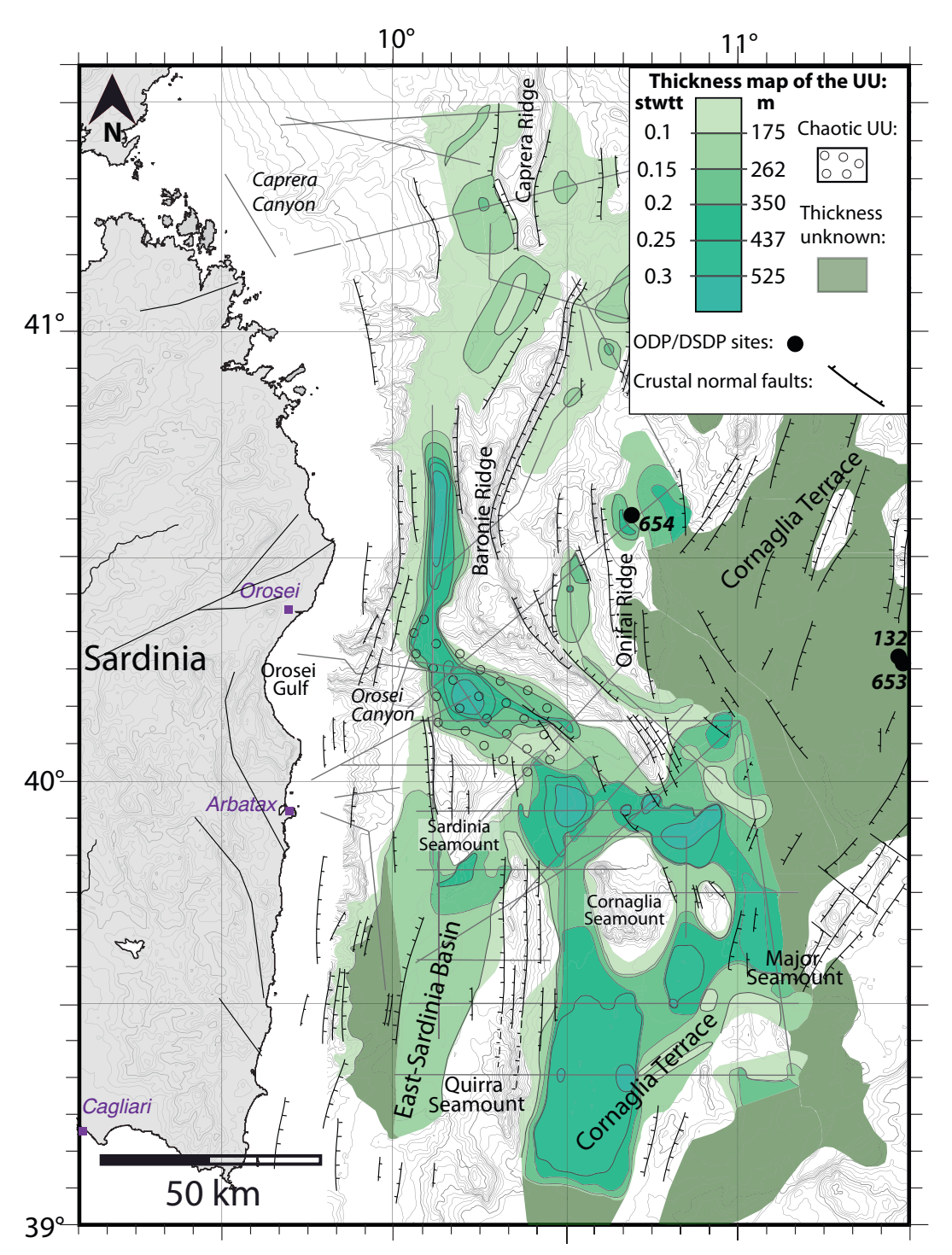
10°
11°
41°
40°
39°
N
Thickness map of the UU:
stwtt
m
0.1
0.15
0.2
0.25
0.3
175
262
350
437
525
Chaotic UU:
Thickness unknown:
ODP/DSDP sites:
Crustal normal faults:
Caprera Canyon
Caprera Ridge
Baronie Ridge
Onifai Ridge
654
Cornaglia Terrace
132
653
Orosei
Sardinia
Orosei Gulf
Orosei Canyon
Arbatax
Sardinia Seamount
Cornaglia Seamount
Major Seamount
East-Sardinia Basin
Quirra Seamount
Cornaglia Terrace
Cagliari
50 km

Figure 12

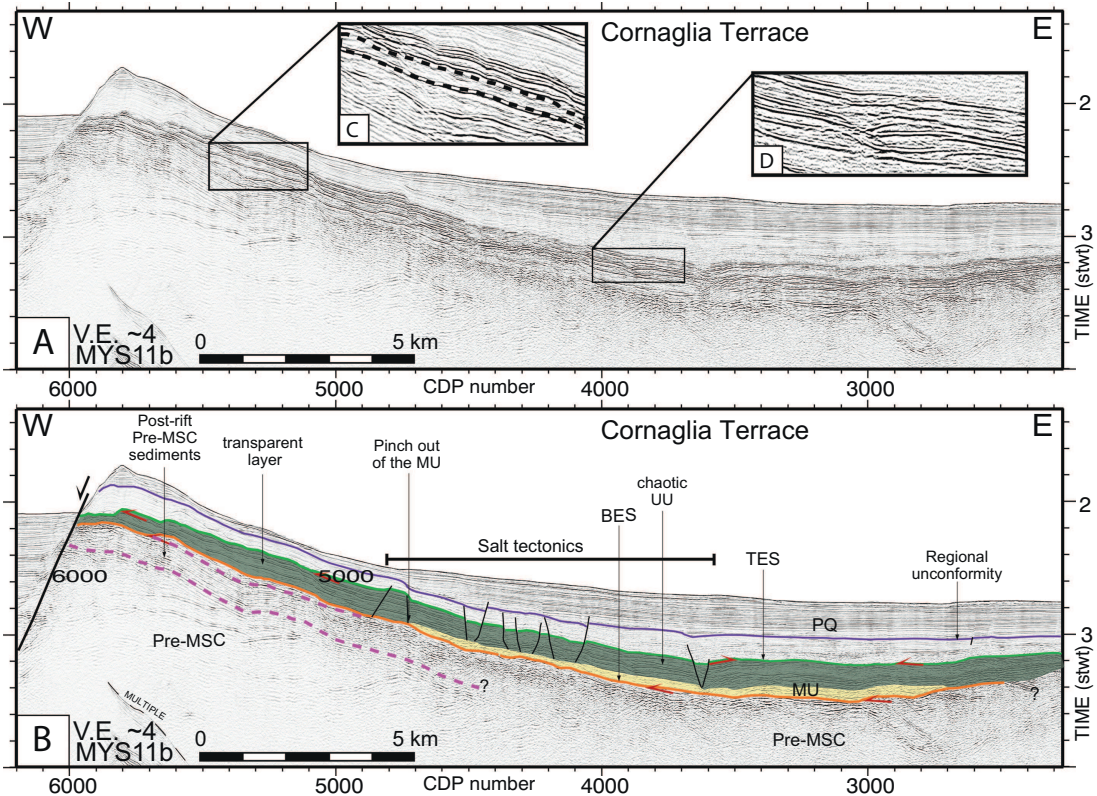
W
Cornaglia Terrace
E
C
D
A
V.E. ~4
MYS11b
0
5 km
TIME (stwt)
2
3
6000
5000
CDP number
4000
3000
W
Post-rift
Pre-MSC
sediments
transparent
layer
Pinch out
of the MU
chaotic
UU
BES
Salt tectonics
TES
Regional
unconformity
Cornaglia Terrace
E
6000
5000
PQ
Pre-MSC
MU
?
MULTIPLE
B
V.E. ~4
MYS11b
0
5 km
Pre-MSC
TIME (stwt)
2
3
6000
5000
CDP number
4000
3000

Figure 13

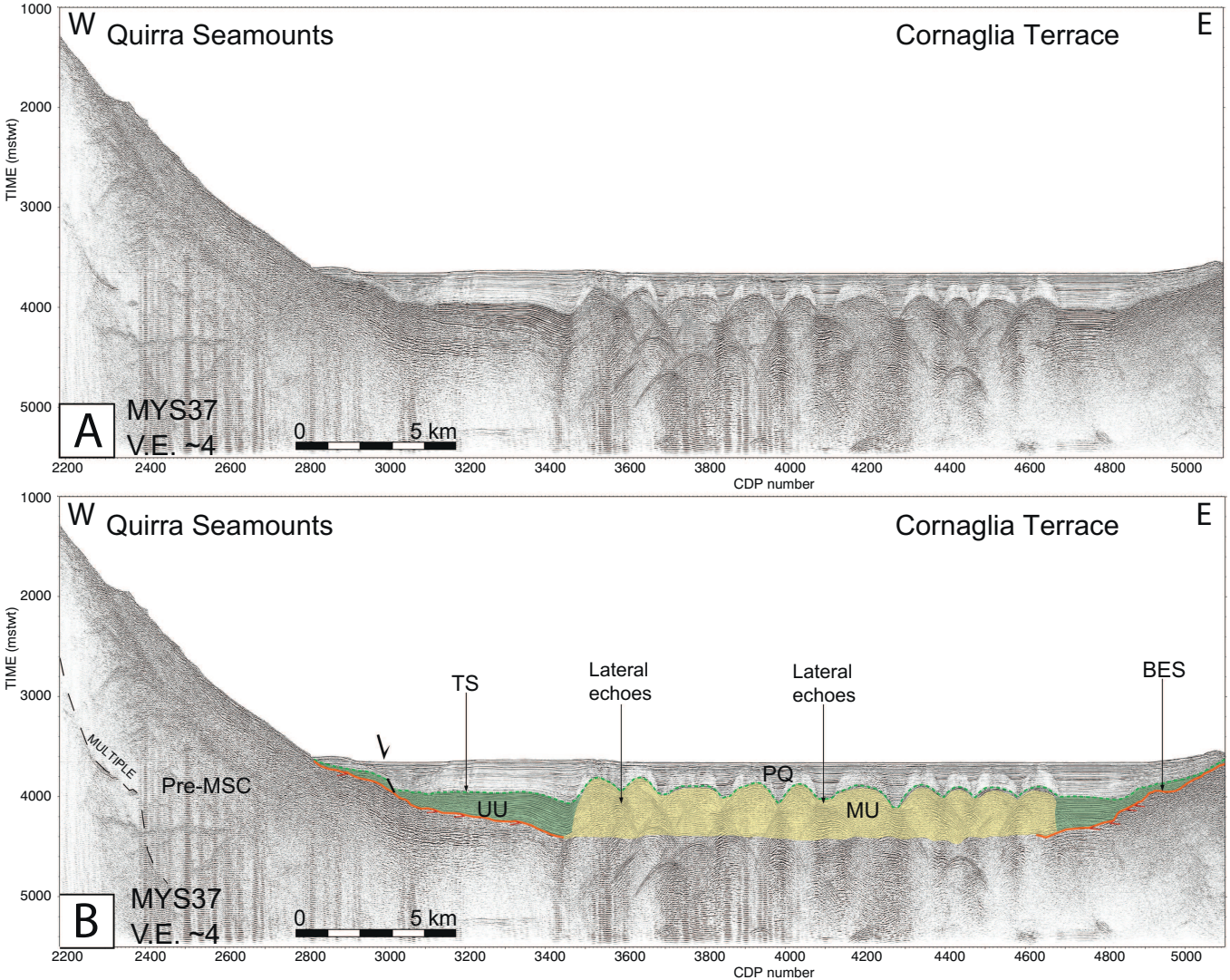
W
Quirra Seamounts
Cornaglia Terrace
E
TIME (mstwt)
1000
2000
3000
4000
5000
A
MYS37
V.E. ~4
0
5 km
2200
2400
2600
2800
3000
3200
3400
3600
3800
4000
4200
4400
4600
4800
5000
CDP number
W
Quirra Seamounts
Cornaglia Terrace
E
TIME (mstwt)
TS
Lateral echoes
Lateral echoes
BES
MULTIPLE
Pre-MSC
UU
PQ
MU
B
MYS37
V.E. ~4
0
5 km
CDP number

Figure 14

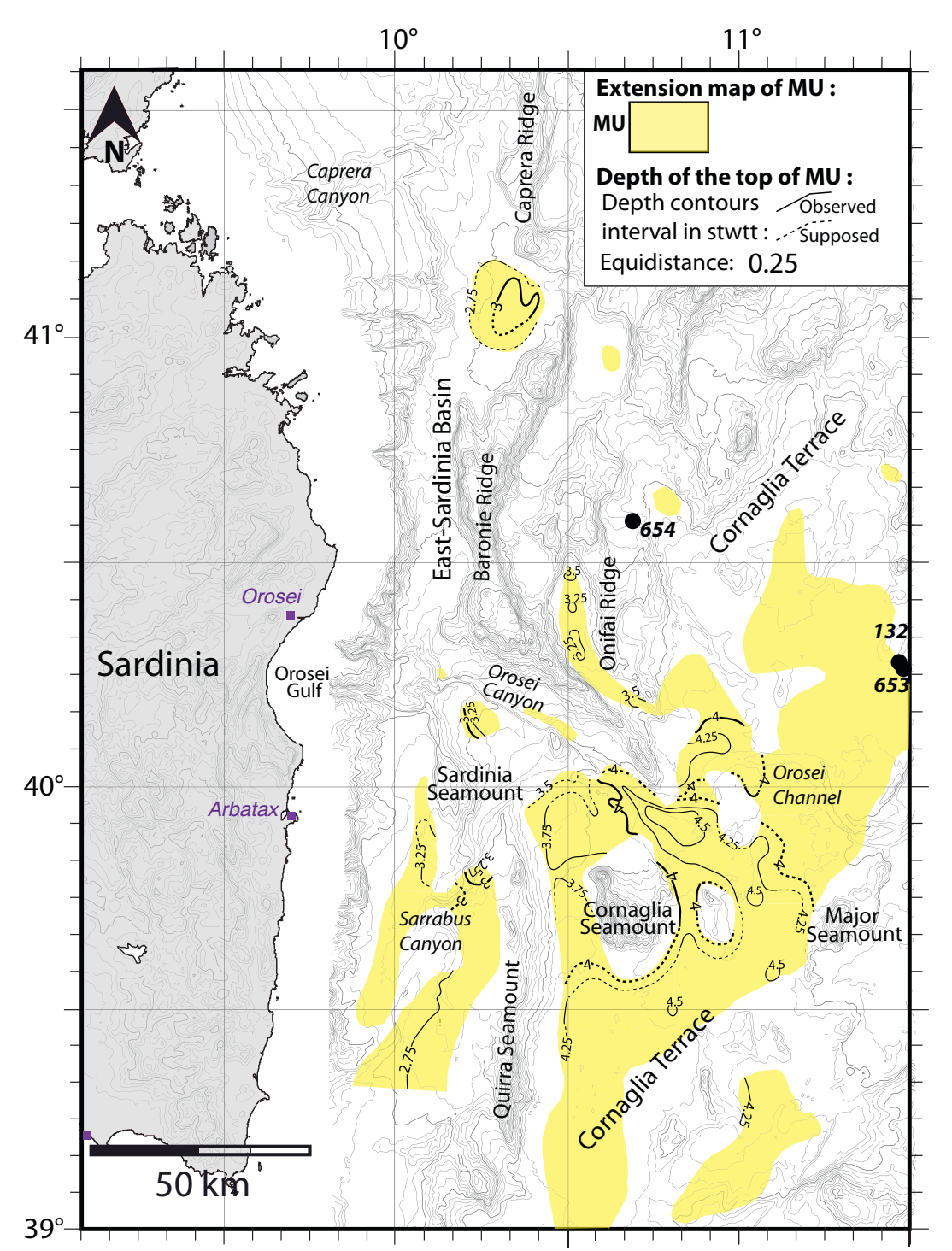
10°
11°
41°
40°
39°
N
Extension map of MU :
MU
Depth of the top of MU :
Depth contours interval in stwtt :
Observed
Supposed
Equidistance: 0.25
Caprera Canyon
Caprera Ridge
East-Sardinia Basin
Baronie Ridge
Onifai Ridge
Cornaglia Terrace
654
132
653
Orosei
Sardinia
Orosei Gulf
Orosei Canyon
Sardinia Seamount
Orosei Channel
Arbatax
Sarrabus Canyon
Cornaglia Seamount
Major Seamount
Quirra Seamount
Cornaglia Terrace
50 km

Figure 15

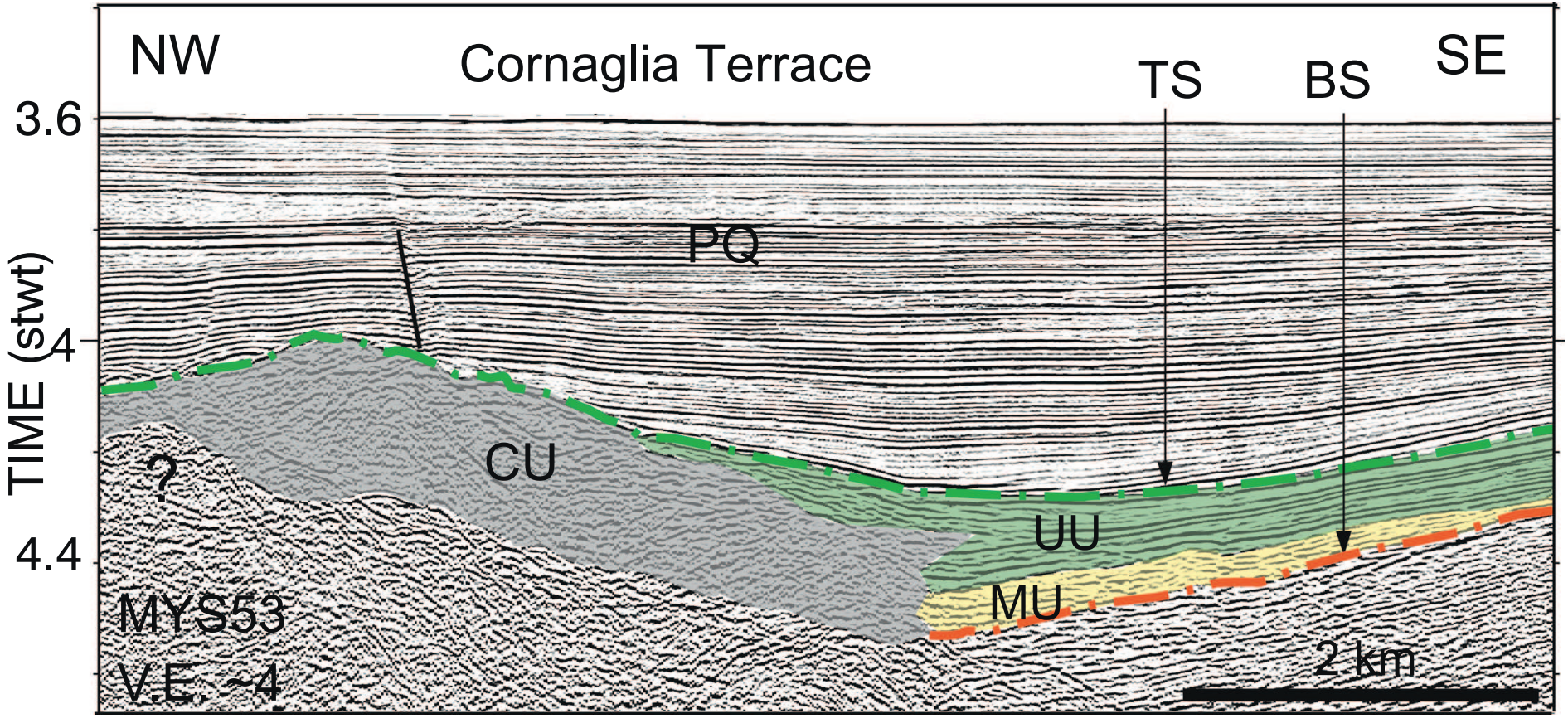
NW
Cornaglia Terrace
SE
TS
BS
3.6
4
4.4
TIME (stwt)
PQ
CU
?
UU
MU
MYS53
V.E. ~4
2 km

Figure 16

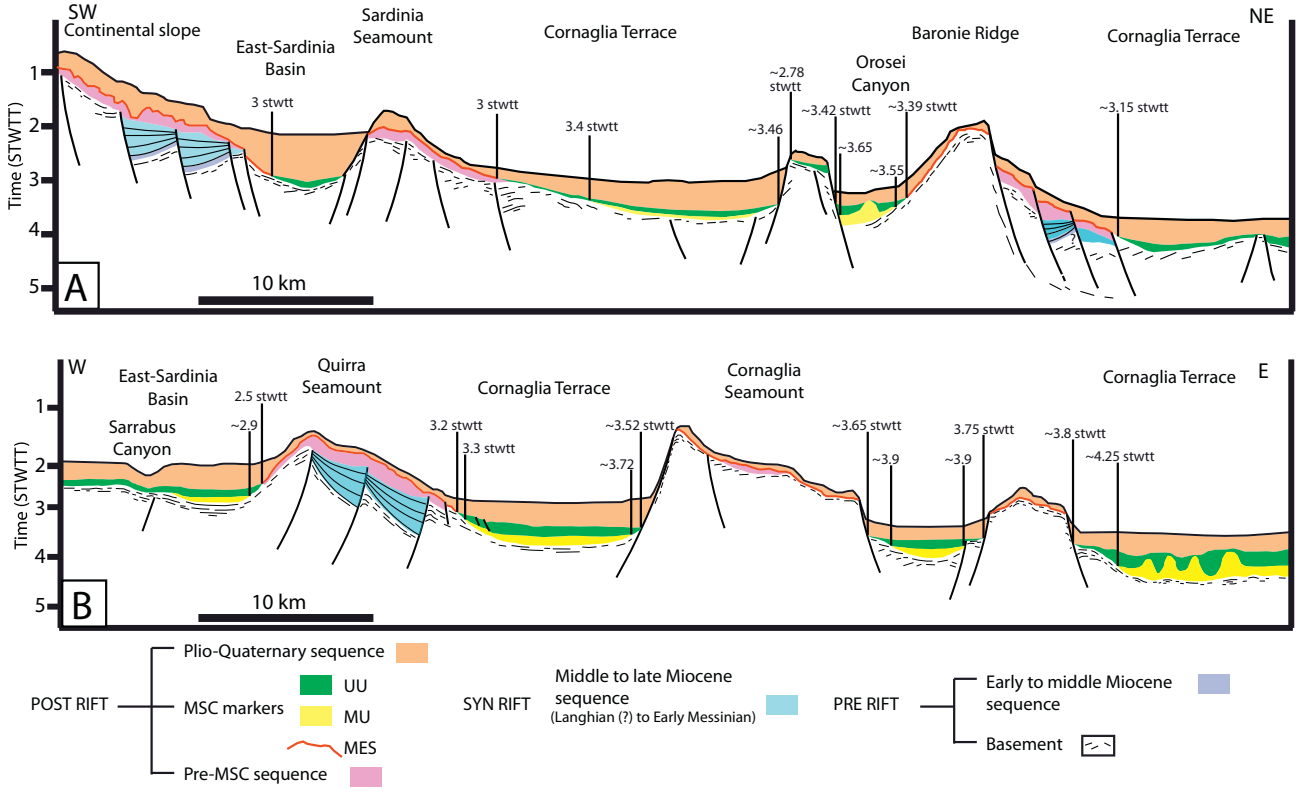
SW
Continental slope
East-Sardinia Basin
Sardinia Seamount
Cornaglia Terrace
Baronie Ridge
Orosei Canyon
Cornaglia Terrace
NE
Time (STWTT)
1
2
3
4
5
3 stwtt
3 stwtt
3.4 stwtt
~2.78 stwtt
~3.46
~3.42 stwtt
~3.65
~3.55
~3.39 stwtt
~3.15 stwtt
A
10 km
W
East-Sardinia Basin
Sarrabus Canyon
Quirra Seamount
Cornaglia Terrace
Cornaglia Seamount
Cornaglia Terrace
E
2.5 stwtt
~2.9
3.2 stwtt
3.3 stwtt
~3.52 stwtt
~3.72
~3.65 stwtt
~3.9
3.75 stwtt
~3.9
~3.8 stwtt
~4.25 stwtt
B
10 km
POST RIFT
Plio-Quaternary sequence
MSC markers
UU
MU
MES
Pre-MSC sequence
SYN RIFT
Middle to late Miocene sequence
(Langhian (?) to Early Messinian)
PRE RIFT
Early to middle Miocene sequence
Basement

Figure 17

MSC SEISMIC MARKERS ACROSS THE ALGERO-PROVENCAL BASIN

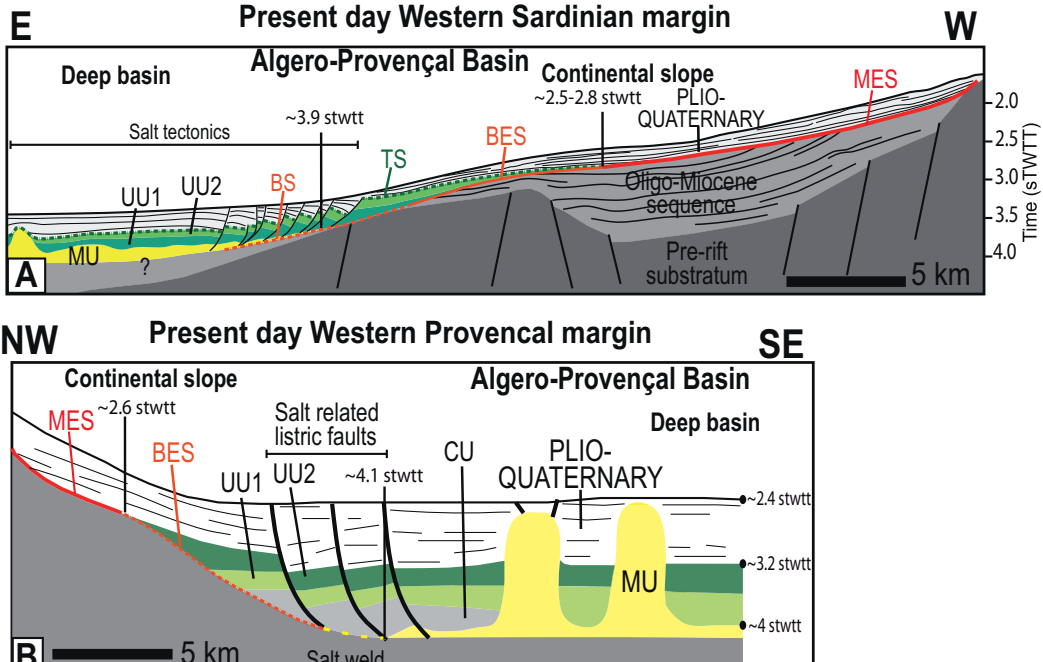

Figure 18